© 2022. Published by The Company of Biologists Ltd | Development (2022) 149, dev201094. doi:10.1242/dev.201094

RESEARCH ARTICLE

EGFR signal transduction is downregulated in *C. elegans* vulval precursor cells during dauer diapause

Catherine O'Keeffe and Iva Greenwald*

ABSTRACT

Caenorhabditis elegans larvae display developmental plasticity in response to environmental conditions: in adverse conditions, second-stage larvae enter a reversible, long-lived dauer stage instead of proceeding to reproductive adulthood. Dauer entry interrupts vulval induction and is associated with a reprogramming-like event that preserves the multipotency of vulval precursor cells (VPCs), allowing vulval development to reinitiate if conditions improve. Vulval induction requires the LIN-3/EGF-like signal from the gonad, which activates EGFR-Ras-ERK signal transduction in the nearest VPC, P6.p. Here, using a biosensor and live imaging we show that EGFR-Ras-ERK activity is downregulated in P6.p in dauers. We investigated this process using gene mutations or transgenes to manipulate different steps of the pathway, and by analyzing LET-23/EGFR subcellular localization during dauer life history. We found that the response to EGF is attenuated at or upstream of Ras activation, and discuss potential membrane-associated mechanisms that could achieve this. We also describe other findings pertaining to the maintenance of VPC competence and quiescence in dauer larvae. Our analysis indicates that VPCs have L2-like and unique dauer stage features rather than features of L3 VPCs in continuous development.

KEY WORDS: *C. elegans*, EGFR, ERK, Ras, Dauer, Vulva

INTRODUCTION

Caenorhabditis elegans larvae display remarkable developmental plasticity in response to environmental conditions, and integrate information about population density, temperature, and food availability to make decisions about developmental progression (reviewed by Baugh and Hu, 2020; Fielenbach and Antebi, 2008; Hu, 2007) (Fig. 1A). In favorable conditions, larvae develop continuously through four larval stages (L1-L4), separated by molts, to become reproductive adults. Adverse conditions in the L1 stage lead to a prolonged second larval stage (L2d), and if they persist, L2d larvae molt into dauer larvae. Although dauer has been called an 'alternative L3 stage', it is a distinct larval state, with morphological and behavioral specializations that facilitate survival and dispersal (Golden and Riddle, 1984). Dauer larvae can survive for several months – many times the lifespan of a worm that develops continuously (Klass and Hirsh, 1976). Favorable conditions induce recovery and developmental progression to reproductive adulthood. Post-dauer worms appear overtly similar to continuously developing worms (Cassada and Russell, 1975), implying the existence of robust protective mechanisms during developmental arrest.

Protective mechanisms include the maintenance of multipotency of precursor cells that give rise to the vulva (Fig. 1B,C). Six vulval precursor cells (VPCs), named P3.p-P8.p. have the potential to generate vulval cells. The specification of the VPCs by cell–cell interactions has provided many important insights into epidermal growth factor (EGF) receptor (EGFR) signaling and its regulation (reviewed by Gauthier and Rocheleau, 2017; Shin and Reiner, 2018; Sternberg, 2005; Sundaram, 2006, 2013). During continuous development, beginning in L2, an EGF signal from the anchor cell (AC) of the gonad activates EGFR and the canonical signal transduction cascade (Ras-Raf-MEK-ERK) in the nearest VPC, P6.p. EGF signaling plays different roles in L2 versus L3. During the L2 stage, EGF and Wnt signaling prevent fusion of P6.p with the hypodermal syncytium (Eisenmann et al., 1998; Myers and Greenwald, 2007). During the L3 stage, EGF signaling induces P6.p to adopt the primary (1°) vulval fate, characterized by expression of EGFR pathway target genes, a distinctive cell division pattern in the L3 stage, and different terminal cell types in the L4 stage.

In dauer life history, the VPCs undergo a reprogramming-like event that preserves their multipotency (Fig. 1D). As first described in mutants that exhibit premature induction of P6.p in the L2 or L2d stages, such that P6.p produces daughters or granddaughters before dauer entry, the lineage does not simply resume after recovery; instead, one of the descendants is induced to adopt the 1° fate by the EGF signal from the AC, suggesting that committed descendants of P6.p are reprogrammed back to a multipotent VPC-like state (Euling and Ambros, 1996). Similarly, in wild type, transcriptional targets of EGFR signaling are expressed in the L2d-dauer molt and then silenced upon dauer entry, suggesting that restoration to multipotency is a normal feature of dauer life history (Karp and Greenwald, 2013).

Dauer development induces changes to gene expression mediated by both global and gene-specific regulation. Global mechanisms are suggested by the observations that dauers have decreased transcription and mRNA abundance overall (Dalley and Golomb, 1992; Snutch and Baillie, 1983), and by changes to the histone landscape implying dauer-specific chromatin remodeling (Hall et al., 2010; Jones et al., 2001). Gene-specific changes are also seen, suggesting that different gene regulatory circuitry is imposed during dauer. For example, dauer alters the complement of microRNAs that regulate the transcription factor HBL-1 (Karp and Ambros, 2012). The reprogramming of VPCs in dauer larvae involves losing expression of transcriptional targets of the EGFR-Ras-ERK pathway (Karp and Greenwald, 2013), which could reflect global or context-specific mechanisms that operate at the level of target gene expression. However, it is unknown whether EGFR-Ras-ERK signal transduction decreases in dauer VPCs to cause silencing exclusively or in parallel to mechanisms that operate at the level of gene expression.

Department of Biological Sciences, Columbia University, New York, NY 10027, USA.

*Author for correspondence (isg4@columbia.edu)

C.O., 0000-0003-0160-7747; I.G., 0000-0001-7180-3706

Handling Editor: Swathi Arur
Received 6 July 2022; Accepted 4 October 2022

Development (2022) 149, dev201094. doi:10.1242/dev.201094

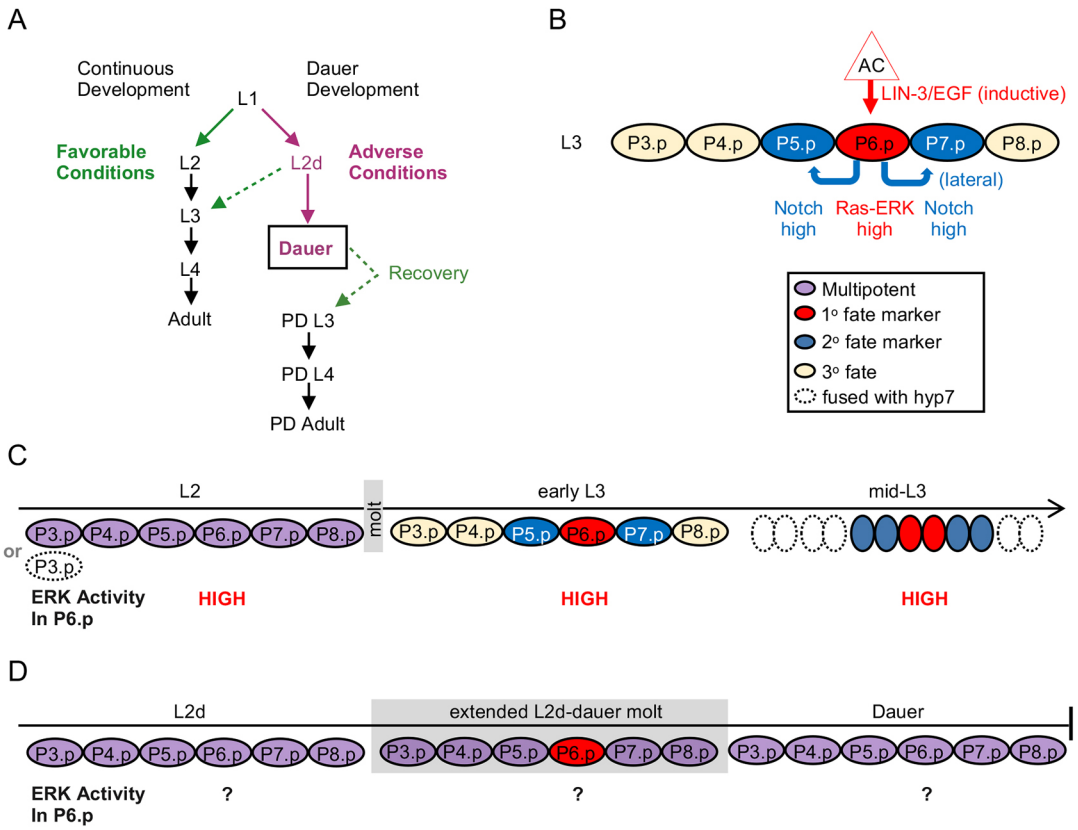

Fig. 1. Life histories and VPC fates. (A) Continuous and dauer life histories. In favorable conditions, *C. elegans* progresses rapidly and continuously through four larval stages separated by molts to reach reproductive adulthood. In adverse conditions, L1 worms molt into an extended pre-dauer L2 stage (L2d). If conditions improve, L2d larvae molt into L3 larvae and continue to develop as in favorable conditions. However, if conditions remain adverse, L2d larvae undergo a prolonged molt and become dauer larvae. If conditions improve, dauer larvae recover and become post-dauer L3 (PD L3) larvae without an intervening molt. The subsequent PD L4 and adult stages are separated by molts. (B) Vulval fate specification. The six multipotent VPCs have the potential to adopt vulval [1° or secondary (2°)] or non-vulval [tertiary (3°)] fates. The AC of the somatic gonad produces an inductive EGF signal and activates EGFR in the closest VPC, P6.p; although this signaling begins in L2, VPC fates are not specified until L3. P6.p adopts the 1° fate, and expresses EGFR-Ras-ERK target genes, including the 1° fate marker *lag-2*, which encodes a ligand for LIN-12/Notch. LAG-2 activates LIN-12/Notch in the neighboring VPCs P5.p and P7.p, specifying them to adopt the 2° fate. The three 'outer' VPCs lack activated EGFR or Notch and adopt the 3°, non-vulval fate. P3.p sometimes fuses with hyp7 in the L2 stage. The key shown also includes symbols for C and D. (C) Sequence of relevant events in continuous development. VPCs are born in L1. During L2, Wnt and EGF signaling promotes VPC 'competence', i.e. prevents their fusion to hyp7. Nevertheless, about 50% of the time, P3.p loses competence and fuses with hyp7 in L2. Although LIN-3/EGF from the somatic gonad activates EGFR signaling and results in high MPK-1/ERK activity in P6.p beginning in L2 (based on ERK-nKTR; de la Cova et al., 2017), the target gene *lag-2* is not expressed until the L2-L3 molt. Transcription of LIN-12/Notch targets is not seen until the L3 stage, when 2° fate is specified. 1° and 2° VPCs undergo characteristic lineages to yield the 22 structural cells of the vulva; only the first division is shown. The two daughters of the 3° VPCs fuse to hyp7. (D) Sequence of relevant events in dauer development. At the outset of this study, it was known that in dauer development, expression of *lag-2* begins during the L2d-dauer molt; crucially, *lag-2* expression is extinguished in dauer, consistent with a natural reprogramming-like event that restores multipotency (Euling and Ambros, 1996; Karp and Greenwald, 2013). It was also known that, during recovery, the VPCs are re-induced, and VPC fate pattern appears indistinguishable from continuous development (Euling and Ambros, 1996). Thus, our first step was to examine ERK activity using ERK-nKTR, as shown in Fig. 2 and characterized thereafter.

Here, we used a genetically encoded biosensor for ERK activity and found that that MPK-1/ERK activation is downregulated in P6.p beginning in the L2d-dauer molt and that activity remains low in dauer larvae. We interrogated the nature of ERK activity downregulation and found that dauer VPCs are profoundly desensitized to EGF despite the presence and correct localization of EGFR in VPCs. In dauer, ERK activity can be increased by an allele that encodes constitutively active Ras, but not by an allele that encodes constitutively active EGFR, suggesting there is a mechanism that prevents EGFR signal transduction at a step upstream of Ras activation. Increasing ERK activity by constitutively activating Ras or Raf does not release VPCs from quiescence and cause them to divide, indicating that desensitization of VPCs to EGF is distinct from, and not the result of, a single global mechanism to prevent VPCs from developmental progression during dauer diapause. Finally, during our analysis, we also found that the gene regulatory circuitry used to maintain VPC competence in dauer differs from that of continuous development. In summary, our analysis indicates that dauer VPCs have some L2-like features rather than L3-like features of continuous development as well as unique features specific to the dauer stage.

RESULTS

The six multipotential VPCs are spatially patterned by differential activation of EGFR and LIN-12/Notch. During wild-type development, P6.p is induced to have a high level of EGFR-Ras-ERK signaling and produces ligands that activate LIN-12/Notch in the neighboring VPCs, P5.p and P7.p. The "outer" VPCs, P3.p, P4.p, and P8.p, do not experience significant activation of either EGFR-Ras-ERK or LIN-12/Notch. In this study, we were primarily

Development (2022) 149, dev201094. doi:10.1242/dev.201094

concerned with the regulation of EGFR-Ras-ERK activity in P6.p during dauer life history, and we used P4.p as a neutral VPC for normalization or comparison as indicated below.

MPK-1/ERK activation is downregulated in VPCs during both the L2d-dauer molt and in dauer

In this study, we used a temperature-sensitive mutant that compromises TGFβ signaling [*daf-7(e1372ts)*, referred to hereafter as *daf-7(ts)*], to drive constitutive dauer formation at 25°C, and corroborated key findings in dauer larvae induced by adverse conditions in a *daf-7(+)* background ('natural dauers'). The use of *daf-7(ts)* greatly facilitates the study of pre-dauer larvae and the examination of animals that have been in dauer for a defined amount of time (Karp, 2018; Larsen et al., 1995; Vowels and Thomas, 1992); *daf-7(ts)* was also used to drive dauer formation in prior studies of VPC quiescence that provided the impetus for this work (Karp and Greenwald, 2013).

To examine EGFR-Ras-ERK signal transduction directly, we used ERK-nKTR, a fluorescent biosensor for quantifying MPK-1/ERK activity *in vivo* (de la Cova et al., 2017), validated in VPCs and other tissues in *C. elegans* (de la Cova et al., 2017, 2020; Maxeiner et al., 2019; Mereu et al., 2020; Robinson-Thiewes et al., 2021). The ERK-nKTR contains a kinase translocation reporter (KTR) containing ERK-dependent phosphorylation sites that promote nuclear export, resulting in cytoplasmic localization of a green fluorescent protein when MPK-1 is active (Fig. 2A), produced from a bicistronic transcript that also encodes a red fluorescent histone protein that marks the nucleus. The red/green ratio of the static red marker to the shuttling green reporter in nuclei is a quantitative measurement of net MPK-1/ERK activity. In continuously developing L2 and L3 larvae, the red/green value is high in P6.p, the VPC closest to the LIN-3/EGF-producing AC, and low in the other VPCs (de la Cova et al., 2017).

We imaged the ERK-nKTR in *daf-7(ts)* dauers at four different time points: L2d, the L2d-dauer molt, ∼2 days into dauer (young dauers) and ∼12 days into dauer (older dauers) (Fig. 2B,C). To compare ERK activity between stages, we normalized ERK activity measured in P6.p to activity measured in P4.p, a cell in which ERK is not activated by the inductive signal (de la Cova et al., 2017). We found that normalized ERK activity in P6.p decreases in wild-type animals during the L2d-dauer molt and remains low in dauer, a phenotype in stark contrast to the persistent, high level of ERK activity specifically in P6.p during continuous development L2 and L3 (de la Cova et al., 2017).

Similarly, we observed strongly downregulated ERK activity in P6.p in dauer larvae that were induced by other treatments. We drove dauer formation using the dauer constitutive temperature-sensitive mutant *daf-2(e1370ts)* [hereafter *daf-2(ts)*], which reduces insulin signaling, and found that ERK activity in P6.p is significantly lower in dauer than in L2d (Fig. 2D), indicating that downregulation of ERK activity is not specific to driving dauer formation by reducing *daf-7*. In addition, ERK activity in P6.p is low in natural dauers compared with continuous development L2 (Fig. 2E), verifying that decreased ERK activity is a property of the dauer state and not a secondary consequence of *daf-7(ts)* or *daf-2(ts)* constitutive dauer formation.

Although ERK activity in P6.p was decreased in dauer, the average ERK activity remained higher in P6.p than in P4.p in all dauer-promoting conditions. This suggested that ERK activity in P6.p is lower during dauer compared with L2d but not completely abrogated. If so, we would expect ERK activation to be further decreased in P6.p, but not in P4.p, in the absence of the EGF-like inductive signal. We removed the inductive signal using the mutant *hlh-2(ar614)*, which carries a deletion of *hlh-2* regulatory sequences and fails to specify an AC (Attner et al., 2019) (Fig. S1) (see Materials and Methods). Indeed, ERK activity in P6.p was significantly lower in *hlh-2(ar614)* AC-less dauers than in wild-type dauers, whereas ERK activity in P4.p was not altered by loss of the AC (Fig. 2F).

Because ERK activity is significantly lower in P6.p in dauer larvae compared with continuous development but is not completely absent, we infer that there is a mechanism that attenuates but does not eliminate either the production of the inductive signal or the response to it. In a previous study, loss of *daf-16*/FOXO in VPCs was found to release P6.p from cell cycle arrest and allow the EGFR-Ras-ERK target gene *lag-2* to be expressed in about half of dauer larvae examined (Karp and Greenwald, 2013). As expected, the inferred mechanism appears to be regulated by *daf-16*, as ERK activity is elevated in *daf-16(0)* dauers (Fig. S2). We therefore proceeded to investigate the level at which such attenuation occurs.

Dauer VPCs are desensitized to LIN-3/EGF

A simple hypothesis to explain low ERK activity in dauer VPCs is that expression of the EGF-like ligand LIN-3 in the AC is downregulated. A transcriptional reporter transgene that has been used historically to assay *lin-3* transcription (Abdus-Saboor et al., 2011; Hwang and Sternberg, 2004) showed bright expression in the AC in natural dauers (Fig. S3A). However, as *lin-3* encodes several predicted isoforms with different regulatory regions, we also wanted to examine endogenous transcription. To do so, we created a synthetic operon by inserting *sl2::nls::TdTomato::nls* immediately after the *lin-3* termination codon, as the last exon is common to all isoforms. This endogenous transcriptional reporter, *lin-3(ar656[lin-3::sl2::nls::TdTomato::nls])*, is expressed in the four proximal gonadal cells that are initially competent to become the AC and remains bright in the AC in *daf-7(ts)* constitutive dauers and natural dauers (Fig. 3A, Fig. S3B,D), indicating that transcriptional regulation of *lin-3* is not the proximate cause for ERK activity downregulation in dauer larvae.

To test potential post-transcriptional levels of regulation, we used heterologous sequences to drive high-level expression of two different forms of LIN-3 in all somatic gonad cells (Fig. 3B). One is the natural transmembrane LIN-3 isoform S ['LIN-3(S)'], which efficiently rescues vulval formation in a *lin-3(0)* mutant (Pu et al., 2017); the other is an engineered secreted EGF moiety ['LIN-3(EGF)'] that is sufficient to activate EGFR signaling in VPCs (Katz et al., 1995), and should bypass any potential requirement for proteolytic processing of a transmembrane EGF precursor in the AC. For these experiments, we used tissue-specific expression of Cre recombinase (*ckb-3p::Cre*) to excise a *flexon* stop cassette (Shaffer and Greenwald, 2022), thereby enabling expression of *lin-3* under the strong ubiquitous *rps-27* (ribosomal protein) promoter specifically in all 12 cells of the somatic gonad primordium in dauer larvae (Fig. 3C, Fig. S3E). Strong expression of LIN-3(S) or LIN-3(EGF) from the somatic gonad in continuous development resulted in a highly penetrant multivulva (Muv) phenotype due to P4.p and other 'outer' VPCs ectopically adopting vulval fates in response to excess ligand, confirming that these ligands effectively activate EGFR-Ras-ERK signaling (Fig. 3D). In contrast, in dauer larvae, these forms of LIN-3 did not result in ectopic activation of ERK in P4.p or increased ERK activity in P6.p compared with 'wild-type' control dauers (Fig. 3E). These observations suggest that dauer VPCs are not readily responsive to ligand produced by the gonad even when the expression level is increased above the endogenous level.

Development (2022) 149, dev201094. doi:10.1242/dev.201094

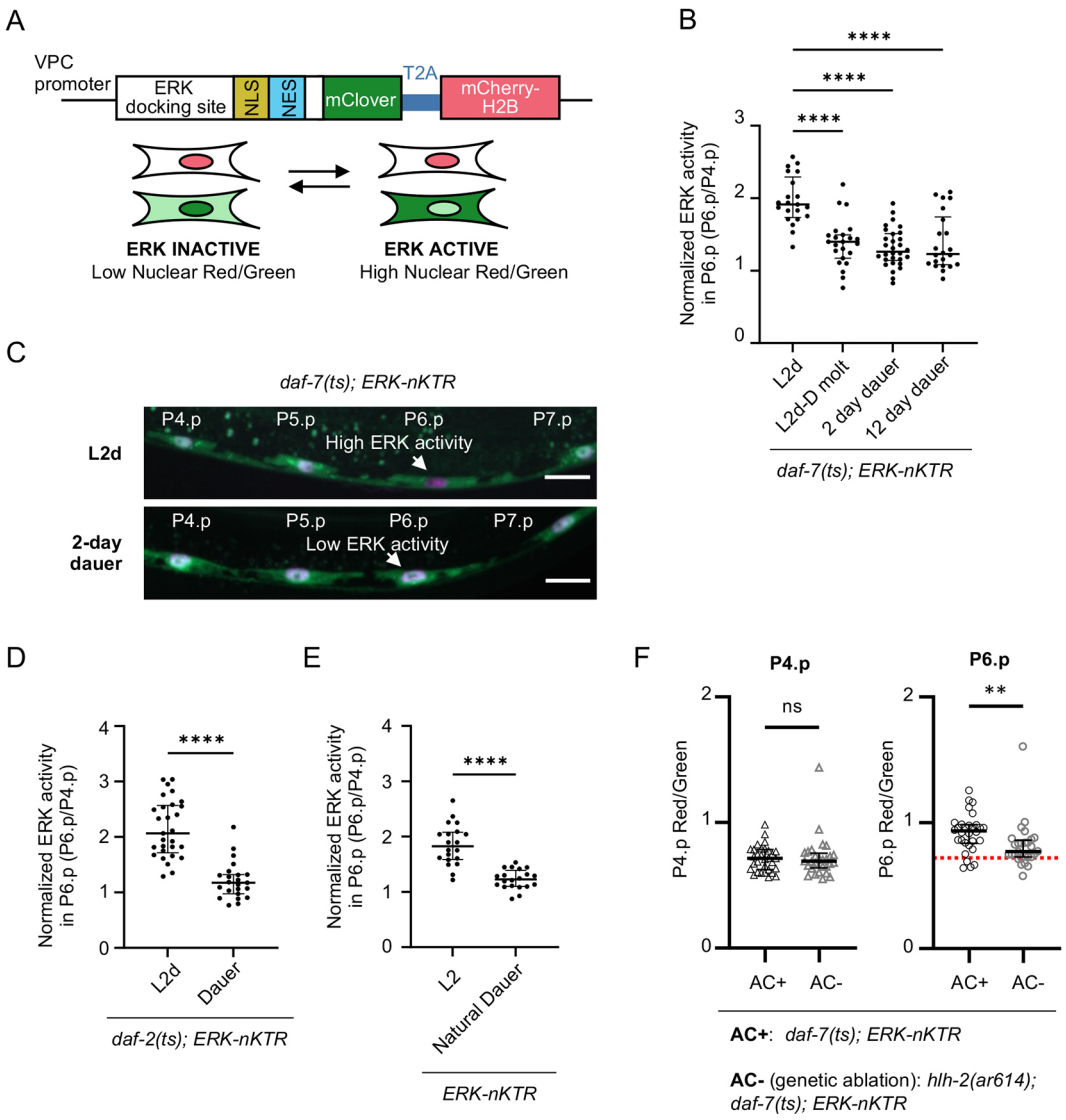

Fig. 2. ERK activity in P6.p decreases in the L2d-dauer molt and in dauer. (A) Schematic (not to scale) of the ERK-nKTR transgene and subcellular localization of mClover as a readout of net ERK activity (de la Cova et al., 2017). When ERK is inactive, the KTR is not phosphorylated and mClover localizes to the nucleus, giving a low nuclear red/green ratio. When ERK is active, phosphorylation of the KTR causes mClover to be exported from the nucleus, giving a high nuclear red/green ratio. (B) Normalized ERK activity in P6.p at different stages in dauer life history in a *daf-7(ts)* background. ERK activity in P6.p was normalized to ERK activity in P4.p on a per-animal basis (P6.p/P4.p; black circles) as the red/green baseline changes over time [L2d (n=21); L2d-dauer molt (n=23); 2-day dauer (n=30); 12-day dauer (n=22)]. The genotype here and in C is *daf-7(ts); ERK-nKTR* (see Table S1 for genotype details and Materials and Methods for staging details). Bars show the median and interquartile range. (C) Maximum intensity projection images from confocal stacks of VPCs in L2d and in a 2-day dauer from B. The genotype of both animals is *daf-7(ts); ERK-nKTR*. The dauer was SDS-selected. Images were autoscaled in ImageJ. Scale bars: 10 µm. (D) Normalized ERK activity in L2d and dauer in a *daf-2(ts)* background, with compromised insulin signaling [L2d (n= 29); dauer (n=23)]. (E) Normalized ERK activity in natural dauers, driven by environmental conditions and not by *daf* mutations (see Materials and Methods) (n=20). Normalized ERK activity in continuously developing L2 larvae is shown for comparison (n=20). (F) Evidence for a low-level of activity in P6.p in dauer. Comparison of ERK activity in P4.p (left; empty triangles) and P6.p (right; empty circles) when there is an AC present (AC+; black) (data from the same 2-day dauers shown in B, n=30) and when the AC is genetically ablated (AC−; gray) (data from the same 2-day dauers shown in Fig. S1A, n=28). The red/green ratio of each cell is not normalized because the comparison is between different VPCs within the same stage (see Materials and Methods). The dashed red line represents the median red/green value in P4.p in AC+ animals during dauer to serve as a baseline reference. **P<0.01 ****P<0.0001 (in B, Kruskal–Wallis test with Dunn's multiple comparisons to compare L2d stages shown with a comparison line: in D-F, Kolmogrov–Smirnov test (see Table S4 and Materials and Methods). ns, not significant.

We also considered whether changes to the basement membrane of the somatic gonad or the pseudocoelomic basal lamina might prevent the EGF signal from reaching EGFR on the VPCs. To test this possibility, we examined *lin-15(n309)*, a mutant in which LIN-3 is expressed ectopically in the major hypodermal syncytium, hyp7 (Cui et al., 2006), on the same side of the pseudocoelomic cavity as the VPCs. Using the endogenous transcriptional reporter *lin-3(ar656)*, we confirmed that *lin-15(n309)* leads to ectopic *lin-3* transcription in hyp7 in dauer (Fig. S3F). We then found that *lin-15(n309)* did not result in ectopic activation of ERK in P4.p in dauer or significantly increase activity in P6.p (Fig. 3F), suggesting that a basement membrane barrier is not the likely reason that VPCs fail to respond to EGF produced from the AC in dauer.

Development (2022) 149, dev201094. doi:10.1242/dev.201094

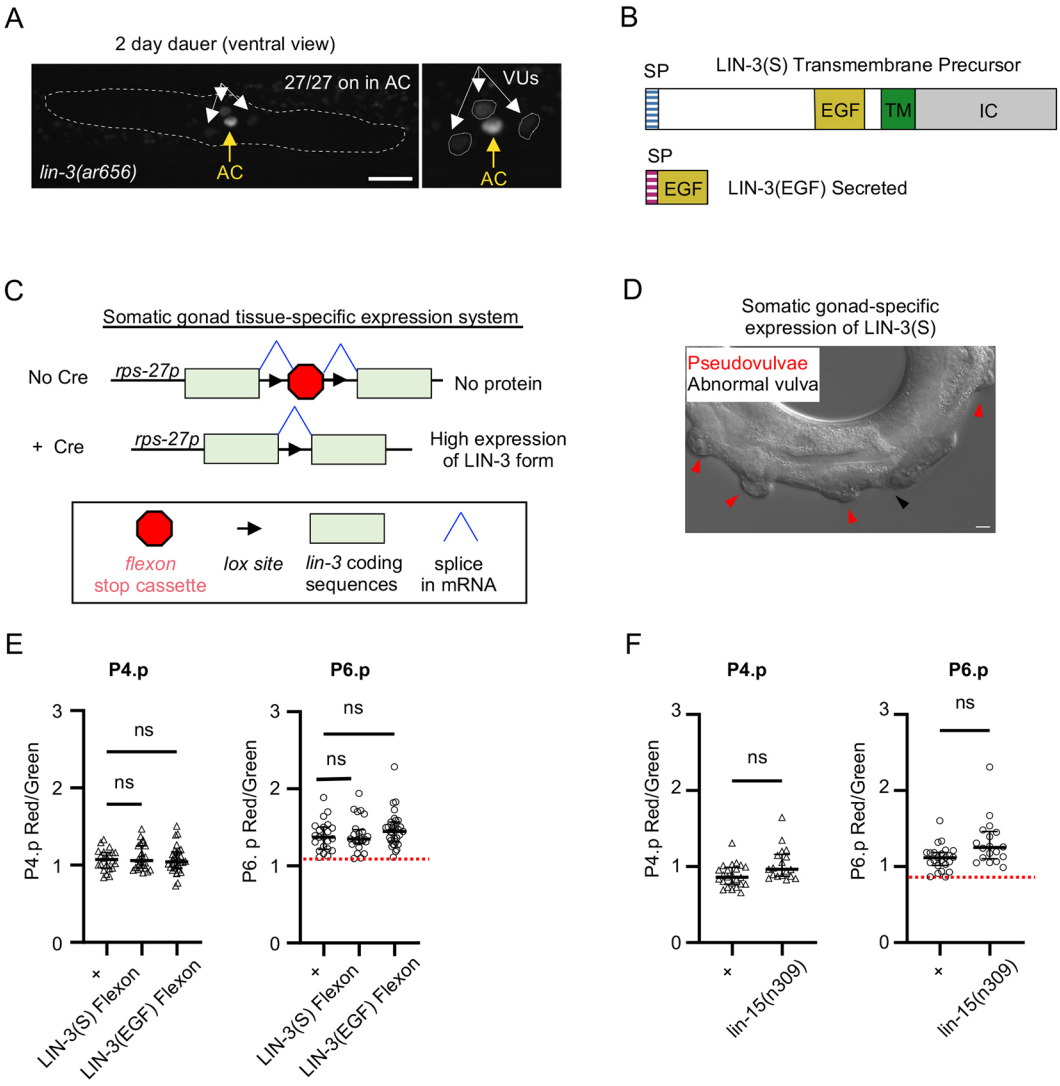

Fig. 3. VPCs are desensitized to LIN-3/EGF. For comparisons here and in Fig. 5, 'wild type' (+) refers to dauers that carry only *daf-7(ts)* and the ERK-nKTR transgene and no additional transgenes or mutations. Noted mutant alleles or transgenes are in a *daf-7(ts)* and ERK-nKTR background (see Table S1 for full genotypes). (A) The LIN-3 transcriptional reporter *lin-3::sl2::nls::TdTomato::nls* [*lin-3(ar656)*] is expressed strongly in the AC and weakly in ventral uterine precursor cells (VUs) in dauers. *hlh-2(ar623[HLH-2::GFP])* was used for cell identification in *hlh-2(ar623); daf-7(ts); lin-3(ar656)* dauers. The somatic gonad is outlined, with the yellow arrow pointing to the AC, and the white arrows pointing to the VUs. the image is a maximum intensity projection of a confocal *z*-stack, autoscaled in ImageJ. Scale bar: 10 µm. Right-hand panel shows an enlarged section of the left-hand image showing bright TdTomato expression in the AC. VUs are outlined. (B) Two forms of LIN-3 that have been shown to activate EGFR-Ras-ERK in VPCs. The first, 'LIN-3(S)' (Pu et al., 2017), is encoded by a cDNA for the S isoform transmembrane precursor protein. The second, 'LIN-3(EGF)' contains a synthetic signal sequence and the EGF domain (Katz et al., 1995). SP (blue stripes), natural signal peptide; SP (pink stripes), synthetic signal peptide; EGF (yellow), EGF domain; TM (green), transmembrane domain; IC (gray), intracellular domain. Not to scale. (C) Somatic gonad-specific expression system. Single-copy insertion transgenes contain constructs in which *rps-27p* drives expression of either LIN-3(S) or LIN-3(EGF); each coding sequence is interrupted by insertion of a *flexon* stop cassette, an artificial exon that leads to nonsense-mediated decay or truncated protein production ('No Cre'). When Cre recombinase is expressed in Z1 and Z4 ('+ Cre'), the *flexon* is excised, resulting in high expression of LIN-3(S) or LIN-3(EGF) in all somatic gonad cells. (D) Somatic gonad expression of LIN-3(S) in continuous development causes a Muv phenotype. The presence of pseudovulvae in adults indicates that EGFR-Ras-ERK signal transduction was ectopically activated in 'outer' VPCs, demonstrating high ligand activity. The balance between EGFR and Notch signaling also appears to be perturbed, leading to an abnormal vulva (Sundaram, 2004). Scale bar: 10 µm. (E) ERK activity in P4.p (left) and P6.p (right) is not elevated when LIN-3(S) or LIN-3(EGF) is expressed from somatic gonad cells. Here and in F, because we compared animals of the same stage and overexpression of EGF affects all VPCs, we directly compared red/green values of a given VPC in the presence of the Flexon overexpression condition with a 'wild-type' (+) control, i.e. animals with the genotype *daf-7(ts); ERK-nKTR* but without the transgenes that cause ectopic EGF production [+, *n*=22; LIN-3(S), *n*=24; LIN-3(EGF), *n*=31]. The dashed red lines on the P6.p graphs for E and F represent the median P4.p ERK activity value of the wild type to serve as a baseline reference. (F) ERK activity in P4.p and P6.p in *lin-15(n309)* mutants, which have ectopic *lin-3*/EGF expression from the hypodermis, compared with wild type [+, *n*=24; *lin-15(n309)*, *n*=18]. In E,F, Kolmogrov–Smirnov test was used to compare each mutant with the wild type of the same experiment. In F, the *P*-value for + versus *lin-15(n309)* in P6.p is <0.05; however, we only considered $P<0.01$ to be significant (discussed in Materials and Methods). ns, not significant.

LET-23/EGFR is present at the basolateral membrane of VPCs in dauer larvae

VPCs are polarized epithelial cells. LET-23/EGFR trafficking and localization are regulated during continuous development, and altering these processes affects signaling strength. Importantly, the default localization of the receptor is the apical membrane, and its trafficking to the basolateral membrane, facing the EGF-producing AC, is crucial for signaling (Kaech et al., 1998). Therefore,

Development (2022) 149, dev201094. doi:10.1242/dev.201094

we examined the expression and localization of LET-23 in P6.p in dauer larvae to determine whether a change in the overt level or subcellular localization of the receptor may underlie the downregulation of ERK activity. We note that expression of DLG-1::RFP, which localizes to the *C. elegans* apical junction (CeAJ), appears similar in both L2d and dauer (Fig. S6) (Diogon et al., 2007), suggesting that the cells maintain their intrinsic apical-basolateral polarity.

Endogenously tagged LET-23 is difficult to visualize in VPCs in live worms (Gauthier and Rocheleau, 2021a). We therefore used *zhIs035*, which overexpresses LET-23::GFP and has been used to examine trafficking of LET-23 in several studies and recapitulates the pattern seen using antibody staining of fixed worms; thus, the degree of LET-23::GFP overexpression does not appear to interfere with normal trafficking while facilitating its detection in live worms (Haag et al., 2014; Skorobogata et al., 2014). In continuous development, basolateral versus apical trafficking of LET-23::GFP in the L2 and L3 stages has been quantified as a ratio of basal/apical peak fluorescence intensity (B/A) (Gauthier and Rocheleau, 2021a,b).

Adapting this method, we examined LET-23::GFP distribution in P6.p during continuous (L2, the L2-L3 molt, and L3) and dauer (L2d, the L2d-dauer molt, and dauer) development. In continuous development, our average B/A values were consistent with the measurements of Gauthier and Rocheleau (2021a) for the L2 and L3 stages. We found a decrease in average B/A LET-23::GFP from L2 to L3 (Fig. 4A-D). In dauer development, the B/A ratio in L2d was very similar to the B/A ratio of continuous L2, and there was a decrease in the B/A ratio during the intervening L2d-dauer molt. However, in dauer larvae, the average B/A LET-23::GFP ratio increased to a value comparable to L2d. We interpret these results as suggesting that a persistent, lower B/A ratio is associated with VPC developmental progression. Furthermore, we speculate that the return to a higher B/A ratio in dauer reflects a return to an 'L2-like' multipotent state, consistent with a reprogramming event. These results indicate that simple loss of LET-23 at the basolateral membrane is not responsible for decreased sensitivity to EGF ligand and downregulation of ERK activity.

Constitutive activation of LET-60/Ras and LIN-45/Raf, but not LET-23/EGFR, is sufficient to increase ERK activity in P6.p in dauer larvae

To gain insight into the mechanism of ERK activity downregulation in dauer, we tested whether mutations that result in strong constitutive activity of EGFR, Ras or Raf in continuous development can increase ERK activity in dauer VPCs. We reasoned that constitutively activating a component at or downstream of the step at which ERK activity is downregulated should increase ERK activity in dauer.

In continuous development, *let-23(sa62)* results in ligand-independent, constitutive activity of LET-23/EGFR, termed 'EGFR(Act)' here. This mutation results in strong constitutive activity in continuous development, even in the absence of the gonad (Katz et al., 1996). Although the biochemical mechanism by which this mutation causes constitutive activity is not clear, the critical observation for this study is that, in contrast to continuous development, we did not observe increased ERK activity in P6.p in EGFR(Act) dauers compared with 'wild-type' control dauers, implying that EGFR(Act) constitutive activity is opposed in dauer (Fig. 5A). In contrast, a mutation that constitutively activates Ras, *let-60(n1046)* [Ras(Act)], and a transgene that expresses

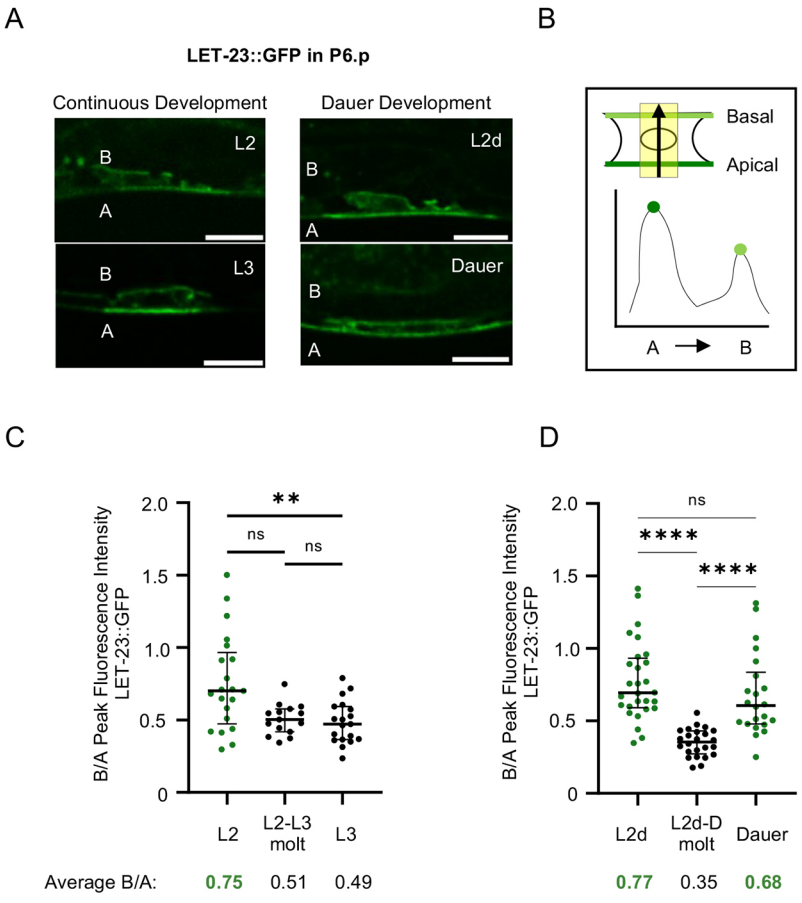

Fig. 4. EGFR localization is 'L2-like' rather than 'L3-like' in dauer larvae. (A) Expression of LET-23::GFP (*zhIs035*) in P6.p. Images are single slices of confocal images, autoscaled in ImageJ. A, apical; B, basal. Scale bars: 10 µm. (B) Peak basal and apical LET-23::GFP values were obtained by drawing a thick line (yellow) through the nucleus, plotting the average fluorescence intensity across the width of the line, and extracting the peak value at the apical membrane and the basal region of the basolateral membrane (see Materials and Methods). (C) Peak basal/apical LET-23::GFP in L2 (n=21), the L2/L3 molt (n=15) and L3 (n=19). (D) Peak basal/apical LET-23::GFP in L2d (n=28), the L2d-dauer molt (n=24) and dauer (n=19). Green indicates that the average B/A ratio is similar to 0.75 (L2-like); black that the average B/A ratio is similar to or lower than 0.5 (L3-like). **P<0.01, ****P<0.0001 (Kruskal–Wallis test with Dunn's multiple comparisons to compare all stages with each other within a graph). ns, not significant.

Development (2022) 149, dev201094. doi:10.1242/dev.201094

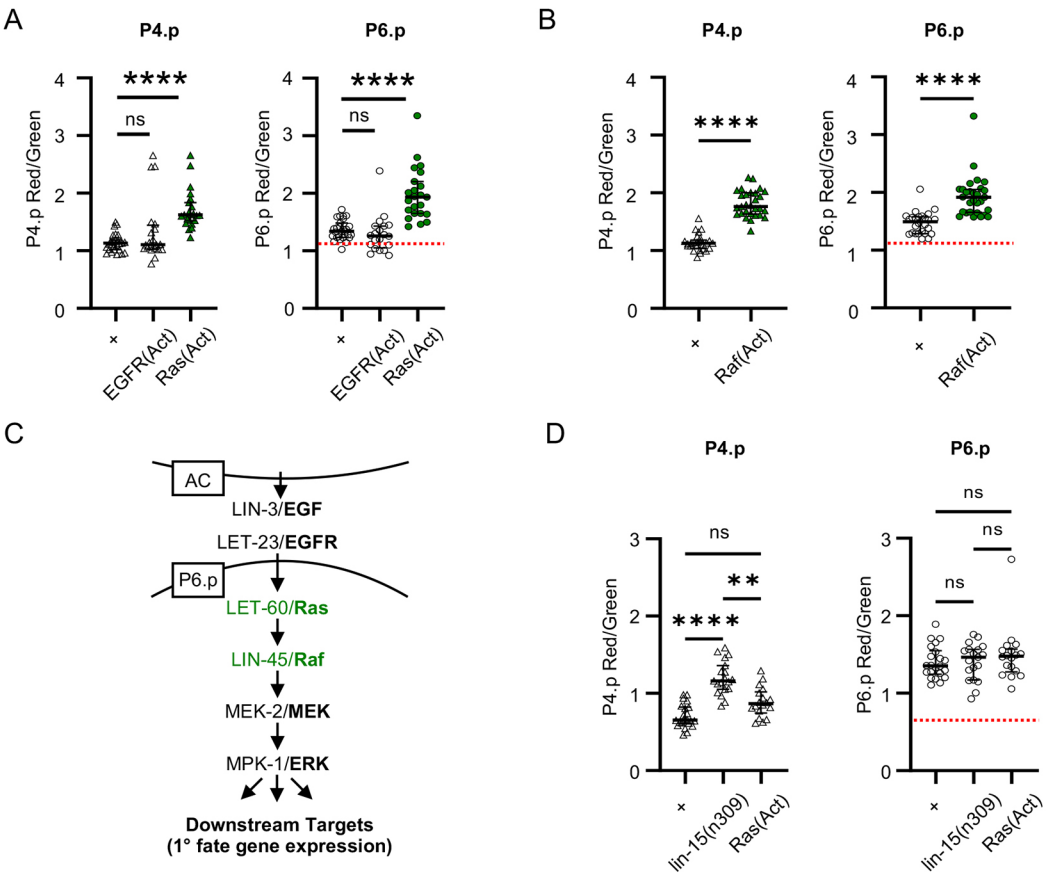

Fig. 5. EGFR signaling is downregulated within the VPCs at or upstream of Ras activation. (A) Comparison of ERK activity in P4.p (left) and P6.p (right) between 'wild type', activated LET-23 [*let-23(sa62)*, 'EGFR(Act)'] and activated LET-60 [*let-60(n1046)*, 'Ras(Act)']. +, *n*=27; EGFR(Act), *n*=20; Ras(Act), *n*=23. All genotypes also include *daf-7(ts)* and *ERK-nKTR*. As constitutive activation of signal transduction potentially affects all VPCs, including P4.p, we compared P6.p red/green values directly without normalizing here and in B and D. Dashed red lines represent the median ERK activity in P4.p of the wild-type group to serve as a baseline reference. Green filled-in dots or triangles represent a genotype that is significantly different from 'wild type' in dauer larvae. (B) Comparison of ERK activity in P4.p and P6.p between 'wild type' and activated LIN-45 [*arTi31* (*lin-31p::lin-45AAE::unc-54), 'Raf(Act)'*]. +, *n*=26; Raf(Act), *n*=29. (C) Schematic view of the EGFR signal transduction pathway. Activation of *let-60* or *lin-45* (green) is sufficient to increase ERK activity in dauer P6.p (A,B). (D) Comparison of ERK activity during L2d, when EGFR signal transduction is not opposed, in both P4.p (C) and P6.p (D). +, *n*=22; *lin-15(n309)*, *n*=19; Ras(Act), *n*=18. ***P*<0.01, *****P*<0.0001 (in A,B, Kolmogrov–Smirnov test to compare each mutant with wild type from the same experiment; in D, Kruskal–Wallis test with Dunn's multiple comparisons to compare all strains to each other within a graph. In D, the *P*-value for + versus Ras(Act) in P4.p is <0.05; however, we only considered *P*<0.01 to be significant (Materials and Methods). ns, not significant.

constitutively active Raf in the VPCs [Raf(Act)] caused increased ERK activity in P6.p (Fig. 5A,B). Furthermore, Ras(Act) and Raf(Act), but not EGFR(Act), also caused ectopic ERK activation in P4.p (Fig. 5A,B). In summary, this analysis indicates that signal transduction is opposed (1) downstream of the step in LET-23 activation that is mimicked by the *sa62* mutation, and (2) at or upstream of Ras activation (Fig. 5C).

Importantly, all genetic manipulations to increase signaling tested here cause highly penetrant Muv phenotypes in continuous development, suggesting that they have comparable effects on pathway activity, and that the different response of VPCs in dauer to activated forms used here is not simply attributable to the intrinsic strength of the alleles or transgenes used. We examined three different conditions that increase EGF signaling: (1) the LIN-3(S) and LIN-3(EGF) flexon transgenes and *lin-15(n309)*; (2) an allele that constitutively activates LET-23; and (3) two different constitutively activated signal transduction cascade components, the Ras(Act) mutation and the Raf(Act) transgene. We found that there is a clean divide: elevating ligand or receptor activity does not activate ERK, whereas elevating Ras or Raf activity does. Together, our analysis implies that dauer-specific downregulation of signaling operates at or upstream of Ras activation and downstream of the step of LET-23 activation mechanism that is elevated by the *let-23(sa62)* mutant. Unfortunately, there are no strongly constitutively active mutants for two conserved pathway components known to link LET-23/EGFR to LET-60/Ras during signal transduction, SEM-5/Grb2 and SOS-1/Sos, so we could not resolve the step at which attenuated signaling occurs further (see also Fig. S5A,B).

We also directly compared ERK activity of *lin-15(n309)*, *let-60(n1046)* and a 'wild-type' control strain in L2d, a stage that should reveal the intrinsic signaling activity of the mutations in animals that are still developmentally progressing but are destined to be dauer larvae. All three strains had indistinguishable levels of ERK activity in P6.p during L2d, suggesting that the maximum activation of the pathway in P6.p had been reached (Fig. 5D). Furthermore, P4.p, the cell that does not normally receive EGF signal, in L2d, had higher ERK activity in *lin-15(n309)* than in *let-60(n1046)* mutants (Fig. 5D), suggesting that *lin-15(n309)* is better able to activate ERK activity in a neutral VPC. However, in dauer, ERK activity in both P4.p and P6.p returned to control levels in *lin-15(n309)* but ERK activity remained increased in *let-60(n1046)*

Development (2022) 149, dev201094. doi:10.1242/dev.201094

(Figs 3F, 5A, Fig. S4). Therefore, the activated position within the signal transduction cascade appears to be more relevant than the 'strength' of the allele.

We also note that we infer that no core component is completely missing, because low ERK activity persists in P6.p (Fig. 2F). However, we were unable to increase ERK activity in P6.p or cause ectopic activation in P4.p (Fig. S5C) by removing negative regulators of EGFR-Ras-ERK signaling that can suppress hypomorphic alleles of pathway components in continuous development, suggesting that the residual signaling in dauer may be lower than in such hypomorphs or that paralogous regulators or other genetic circuits operate in dauer.

Additional insights into reprogramming and competence in the dauer state

Use of the ERK-nKTR to assess ERK activity during recovery from the dauer state has afforded insights into the natural reprogramming-like mechanism that restores multipotency and maintains competence in the dauer state. We described above how ERK activity in L2d parallels the L2, with high ERK activity in P6.p. Differences emerge in the L2d-dauer molt and in dauer itself, when ERK activity decreases and remains low in P6.p, compared with L3, when activity continues to be high. When we examined normalized ERK activity in natural dauers during recovery from the dauer state, we observed that normalized ERK activity was significantly increased in P6.p by ∼6 h into dauer recovery at 25°C (Fig. 6A). In addition, ERK activation occurred before the VPCs divided, mimicking the sequence of events seen in continuous development and consistent with the reinduction of 1° fate after a natural reprogramming-like event restores VPCs to their initial multipotent state (Euling and Ambros, 1996; Karp and Greenwald, 2013).

VPC competence refers to the mechanism that prevents VPCs from fusing to the hyp7 syncytium in the L2 stage, unlike their anterior and posterior Pn.p lineal homologs (reviewed by Sternberg, 2005). In wild type, there is natural variability in the competence of P3.p during continuous development: P3.p fuses to the hypodermis ∼50% of the time in the L2 stage (Delattre and Félix, 2001; Eisenmann et al., 1998; Myers and Greenwald, 2007). Previous work has shown that the division frequency of P3.p is sensitive to environmental conditions (Braendle and Félix, 2008). Inherent properties of ERK-nKTR make it a useful fusion marker: in competent, unfused VPCs, mClover is visible in the cytoplasm of the cell and mCherry-H2B is expressed in the nucleus. When a VPC loses competence and fuses to hyp7, mClover in the cytoplasm disappears as it gets diluted in the syncytium, whereas mCherry-H2B persists in the nucleus (Fig. 6B). Over the course of our analysis using ERK-nKTR, we incidentally observed that P3.p was generally maintained unfused throughout dauer diapause in every genotype scored (Fig. S7). We first ascertained that P3.p still fused without dividing in 50% of worms in continuous development (n=5/10). Therefore, the suppression of P3.p fusion we observed in dauer life history cannot be explained by a difference in genetic background.

During L2, *lin-39* expression in the VPCs, promoted by both Wnt and EGFR signaling, maintains VPC competence (Eisenmann et al., 1998; Myers and Greenwald, 2007). Thus, the observation that P3.p always remains competent in dauer life history raises the question of whether dauer-destined larvae have increased Wnt signaling to help maintain VPC competence, as we already know that EGFR signaling is decreased. To test this possibility, we examined P3.p fusion in a mutant lacking *cwn-1*, which encodes a ligand of the Wnt family that is essential to maintain P3.p competence in continuous

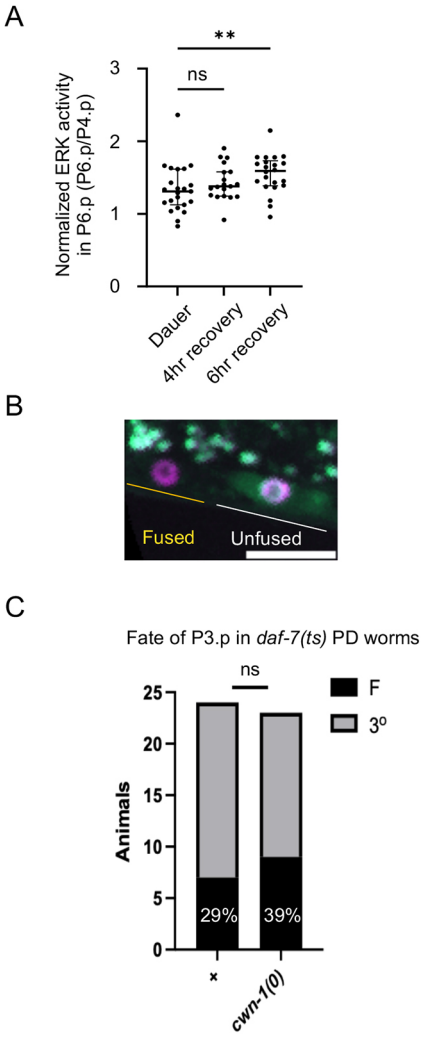

Fig. 6. Reprogramming and competence in dauer larvae. (A) Normalized ERK activity in natural dauers, and at defined times after dauer recovery was induced. Dauer, n=23; 4 h after recovery was initiated, n=19; 6 h recovery was initiated, n=22. (B) ERK-nKTR can distinguish VPCs that remain competent from VPCs that have fused with hyp7. When P3.p is unfused, the red-labeled histone is visible in the nucleus and green-labeled KTR is visible in the cytoplasm. When P3.p has fused, green is no longer visible as it gets diluted in the hyp7 syncytium but red in the nucleus remains. Image was autoscaled in ImageJ. Scale bar: 10 µm. (C) The percentage of worms in which P3.p fuses directly without dividing in 'wild-type' and *cwn-1(0)* recovered PD worms. F (black) indicates when P3.p fused directly without dividing and 3° (gray) indicates when P3.p divided once and then fused [+ (n=24); *cwn-1(0)* (n=23)]. **P<0.01. In A, Kolmogrov–Smirnov test to was used to compare post-dauers to dauer; in C, Fisher's exact test to compare + versus *cwn-1(0)*. ns, not significant (P>0.01).

development (Gleason et al., 2006; Myers and Greenwald, 2007). Surprisingly, we found that *cwn-1* is not required to maintain VPC competence in dauer life history: in 48/49 *cwn-1(0) daf-7(ts)* 1- and 2-day dauers, P3.p remained unfused. This observation suggests that there may be another Wnt that maintains competence in dauer larvae or an alternative mechanism to maintain competence.

When natural dauers made by starvation and crowding were induced to recover, we found that P3.p fused directly with hyp7 in about half of the post-dauer larvae (n=10/24). Therefore, P3.p, which remains competent throughout all of L2d, the L2d-dauer molt, and dauer, behaves as it does in the L2 stage of continuous development, suggesting that reprogramming to multipotency does

Development (2022) 149, dev201094. doi:10.1242/dev.201094

not cause a permanent change in P3.p competence. Surprisingly, though, we found that *cwn-1* is not required to prevent fusion during recovery from dauer (Fig. 6C), indicating that passage through dauer may produce a lasting genetic circuitry change.

DISCUSSION

Using a genetically encoded biosensor for ERK activity, ERK-nKTR, we found that the EGFR-Ras-ERK pathway activity is regulated in VPCs during dauer life history. In L2d, signaling is similar to that in continuous L2, but signaling is downregulated in P6.p during dauer entry, and remains downregulated for the duration of the dauer state. We also found that during dauer the VPCs become desensitized to EGF: excess LIN-3/EGF production from the gonad or ectopic cellular sources is unable to activate signal transduction in VPCs. Similarly, a missense mutation in LET-23/EGFR that causes strong constitutive signaling in continuous development cannot activate signaling in dauer VPCs. In contrast, mutations that cause strong constitutive activity of LET-60/Ras or LIN-45/Raf in continuous development are able to activate signal transduction in dauer. Together, our results indicate that the response to EGF is attenuated at or upstream of Ras activation, and is likely to involve modulation of receptor activity.

Potential mechanisms for attenuating EGFR signal transduction in dauer VPCs

Studies of mammalian EGFR suggest mechanisms that operate at the level of the receptor or cell membrane that could be engaged in dauer VPCs. Two major mechanisms for regulating mammalian orthologs of EGFR are differential stabilization of receptor dimerization (Freed et al., 2017) and increased endocytic trafficking of the receptor to degradative compartments (Sigismund et al., 2008). However, these mechanisms seem unlikely to be relevant to the downregulation of LET-23 signaling we have described here because, unlike its mammalian orthologs, LET-23 is thought to be a constitutive dimer that responds to a single ligand (Freed et al., 2015), and LET-23::GFP is present at the basolateral membrane in dauer larvae. However, three other regulatory mechanisms described in mammalian cells may apply, and potentially could operate alone or redundantly in dauer larvae.

First, in some contexts, receptor tyrosine kinases, including EGFR, have been shown to continue signaling after internalization and downstream core signaling components colocalize in endosomes (Miaczynska and Bar-Sagi, 2010; Platta and Stenmark, 2011). These 'signaling endosomes' may amplify signals or act as RTK signaling platforms (Miaczynska, 2013; von Zastrow and Sorkin, 2007). A recent *C. elegans* study suggested that suppression of certain constitutive endocytosis pathways is a general feature of dauer larvae (Richardson et al., 2019), making it plausible that decreased endocytosis may reduce the ability of a cell to sustain high ERK activity.

Second, parallels between dauer VPCs and aged senescent human diploid fibroblasts (HDFs) suggest that, in dauer, EGFR on the basolateral membrane could be in a microenvironment that is not permissive for signaling. Senescent HDFs are insensitive to EGF (Park et al., 2000), even though the levels of both EGFR and ERK are similar to the levels in young, EGF-responsive cells. Caveolae may play a role in reduced signal transduction, as the level of caveolin is elevated in aged cells, and ectopic expression of caveolin 1 in young HDFs is sufficient to attenuate EGFR signaling (Park et al., 2000). It is not yet clear whether *C. elegans* has caveolae, although *C. elegans* has two caveolin genes, and their products are localized in membrane-associated puncta (Parker et al., 2009; Sato et al., 2006; Sloan and Bembenek, 2020). However, null alleles of caveolin genes do not cause overt vulval defects, so at this time it is an open question as to whether there may be modulatory effect on signal reception, and it is further possible that compensatory mechanisms are induced in null mutant backgrounds.

Finally, the extensive metabolic changes that occur in dauer larvae (Baugh and Hu, 2020) may result in membrane lipid composition unfavorable for signaling, as lipid composition and crowding of the membrane are thought to contribute to Ras nanocluster formation, which concentrates Ras and its downstream effectors to promote efficient signaling (Nussinov et al., 2021; Zhou et al., 2018).

VPCs have L2-like and unique dauer-stage features

When dauer larvae recover, they enter post-dauer L3 (PD L3) without an intervening molt; they subsequently molt into post-dauer L4. The lack of a dauer-PD L3 molt has contributed to the view that dauer is an 'alternative L3 stage', but there are many specializations of dauer anatomy and physiology that make dauer distinct, and the reprogramming-like event was the first indication that there are special mechanisms for preserving quiescence and multipotency of VPCs in dauer (Euling and Ambros, 1996; Karp and Greenwald, 2013). We found that dauer VPCs share more similarities with L2 VPCs than with L3 VPCs, but also have unique characteristics consistent with a unique dauer-stage identity.

We have identified two L2-like features here. First, the distribution of EGFR (LET-23::GFP) in dauer is more L2-like than L3-like. Second, increasing ERK activity by bypassing opposition to signal transduction does not cause cell cycle progression, which parallels the ability of VPCs to sustain high ERK activity in L2 without dividing (de la Cova et al., 2017). In addition, a previous observation about the transcription factor LIN-1/ELK1 may also be viewed as an L2-like feature. LIN-1 is phosphorylated by MPK-1 in response to the inductive signal (Jacobs et al., 1998, 1999; Miley et al., 2004); during continuous development, it is required during the L3 stage, but not the L2, stage, for repression of *lag-2* in VPCs other than P6.p (Underwood et al., 2017; Zhang and Greenwald, 2011). However, in dauer, LIN-1 is no longer required for repression of *lag-2* in VPCs (Karp and Greenwald, 2013), so the lack of a requirement for LIN-1 in dauer may also reflect VPC reprogramming to an 'L2-like' state.

The preservation or restoration of L2-like features after the L2-dauer molt is consistent with a reprogramming event that restores multipotency, a phenomenon that is unique to dauer larvae and is itself evidence for a unique state different from L2 or L3. However, we have identified additional features that suggest that VPCs have a uniquely dauer-stage identity that do not have L2 or L3 counterparts. Our major focus was on regulation of EGFR-Ras-ERK signaling, and we found that, unlike L2, L2d or L3, ERK activity in dauer remains low in dauer even though the EGF signal is present. We also found that, despite the presence of EGFR on the basolateral membrane, the VPCs are desensitized to EGF ligands and to mutational activation of LET-23 that causes a constitutive response in continuous development. Furthermore, we found that there is a difference in the competence of VPCs, as P3.p never fuses with hyp7 in dauer as it would it in about 50% of continuous L2 hermaphrodites, and that CWN-1, a Wnt ligand that is absolutely required for P3.p (and P4.p) to remain competent in L2, is not required to maintain competence in dauer. A better understanding of the dauer state may reveal how quiescence and multipotency are maintained over long periods of time in other animals, and may provide insights into basic features of stem cell biology.

Development (2022) 149, dev201094. doi:10.1242/dev.201094

MATERIALS AND METHODS

C. elegans genetics

A full list of the *C. elegans* strains used in this work can be found in Table S1. Transgenes used can be found in Table S2. Plasmids can be found in Table S3. Statistical tests and *P*-values can be found in Table S4. Some strains and transgenes were provided by the Caenorhabditis Genetics Center (CGC) at the University of Minnesota. The N2 Bristol *Caenorhabditis elegans* strain was used as the starting strain for all crosses and injections. Strains were maintained on *Escherichia coli* OP50; all strains were maintained at 15°C (due to temperature-sensitive dauer-constitutive mutations) and experiments were performed at 25°C as described below.

The following previously published alleles and single-copy insertion transgenes were used in this study: *daf-7(e1372ts)* and *daf-2(e1370ts)* cause constitutive dauer formation at 25°C (Karp, 2018; Larsen et al., 1995; Vowels and Thomas, 1992); *hlh-2(ar614)* has a small deletion ∼5 kb upstream of the coding region that removes *hlh-2* expression specifically from the proximal gonad (Attner et al., 2019) such that an AC is not specified [additionally, *hlh-2* is required for expression of *lin-3* in the AC (Hwang and Sternberg, 2004); therefore, this allele effectively acts as a null allele of *lin-3*/EGF for vulval induction (Fig. S3C)]; *hlh-2(ar623)* was generated by CRISPR/Cas9-mediated genome engineering and encodes GFP::HLH-2 (Attner et al., 2019); *let-23(sa62)* [EGFR(Act)] encodes a constitutively activated receptor as a result of a point mutation in the extracellular cysteine-rich domain, near the major ligand-binding domain (Katz et al., 1996); *let-60(n1046)* [Ras(Act)] encodes a constitutively activated Ras protein caused by point mutation that may favor maintenance of the Ras-GTP active state (Beitel et al., 1990); *lin-15(n309)* results in ectopic expression of *lin-3* from the major hypodermal syncytium, hyp7, and other cells (Cui et al., 2006; Fig. S3F); the negative regulators of EGFR-Ras-ERK signaling tested were *gap-1(ga133)* (Hajnal et al., 1997), *dep-1(zh34)* (Berset et al., 2005), *lip-1(ok154)* (Das et al., 2022) and *sli-1(sy143)* (Yoon et al., 1995), which are all predicted to be null or strong loss of function alleles; *sos-1(pd10)* is a missense mutation isolated as a suppressor of *sem-5(n1619)* lethality, but has no phenotype on its own (described by Pu et al., 2017); *daf-16(mgDf50)* is a large deletion and is predicted to be a molecular null allele (Ogg et al., 1997); *cwn-1(ok546)* (C. elegans Deletion Mutant Consortium, 2012) contains a large deletion and is predicted to be a molecular null allele (Zinovyeva and Forrester, 2005); *arTi31* [Raf(Act)] is a single-copy insertion transgene that expresses an activated and stabilized form of LIN-45 in the VPCs [*lin-31p::lin-45(T432A, S436A, V627E)::unc-54 3′UTR*] (de la Cova et al., 2017); we used two ERK-nKTR single-copy insertion transgenes, *arTi87* and *arTi85*, that express the ERK-nKTR biosensor in the VPCs (de la Cova et al., 2017, 2020) and are identical except for their insertion site (wild-type controls for a given experiment always carried the same ERK-nKTR transgene as mutants).

Identifying and scoring dauer larvae and other stages in dauer life history

In this work, we looked at hermaphrodite dauers formed using mutations that result in constitutive dauer formation or at dauers isolated from starved and crowded plates (‘natural dauers’). Unless otherwise noted, all dauers were isolated by 1% SDS selection before scoring, the most stringent test of dauer formation, and assessed for dauer characteristics, such as radial constriction and alae formation.

Strains were maintained at 15°C, the permissive temperature for dauer-constitutive mutations. To score dauer larvae in *daf-7(e1372ts)* strains, worms and eggs were washed off continuously growing plates and treated with sodium hydroxide and bleach to isolate eggs. Eggs were plated on an OP50-seeded plate and shifted to 25°C to induce dauer formation. Unless otherwise noted, dauers were scored ∼96 h after egg preparation, when the animals had been in dauer for approximately 2 days (‘2-day dauers’). For scoring *daf-2(e1370ts)*, which develop more slowly than *daf-7(e1372ts)*, we scored ∼120 h after egg preparation to ensure worms had been in dauer for at least 2 days. In order to obtain natural dauers, ten gravid hermaphrodites were picked onto an OP50-seeded plate and the plate was incubated at 25°C. By ∼10 days, the food had been consumed and selection with 1% SDS yielded many dauers.

A modified protocol was necessary to isolate *daf-7(e1372ts); let-23(sa62)* and *lin-3(ar656); lin-15(n309)* dauer larvae because the strains were sick and dauers could not be obtained using the above protocol. The strains were maintained at 15°C until crowded and then the crowded plate was shifted to 25°C. Three days later, we performed SDS selection and scored the resulting dauers. We verified that this modified protocol did not have unexpected effects on ERK activity: we assessed *daf-7(e1372ts); arTi87(ERK-nKTR)* and *daf-7(e1372ts); let-60(n1046); arTi87(ERK-nKTR)* dauers using this protocol and obtained the same results as in our usual dauer isolation protocol (Fig. 5A, Fig. S3).

When scoring ERK-nKTR in dauer stages, all mutant or natural dauer larvae were scored within 2 h of 1% SDS selection. Because dauer larvae are very sensitive to the environment, for all experiments in which ERK activity in P6.p was to be compared directly, the control strain was set up and stored in parallel with the experimental strain and scoring was performed back-to-back.

In order to score ERK-nKTR in L2, L2d and the L2d-Dauer molt, tighter synchronization was used. Isolation of eggs was followed by picking worms that hatched within 2-4 h increments. L2 larvae were scored ∼15 h post hatching. L2d larvae were scored ∼20 h post hatching and L2d-Dauer molt larvae were scored ∼30 h post hatching (Karp, 2018). Morphological characteristics were also used to confirm stages such as gonad size, the presence of a buccal plug in the L2d-dauer molt, and a lack of radial constriction. Animals carrying the *daf-7(ts)* mutation still enter a prolonged L2/L2d stage and can sometimes enter dauer at the lower permissive temperature (Swanson and Riddle, 1981; reviewed by Karp, 2018). Therefore, only dauer life history is studied in worms containing the *daf-7(ts)* mutation.

To score recovering dauers, we performed SDS selection to isolate natural dauers, plated them onto fresh OP50-seeded plates, and allowed recovery to occur at 25°C. These animals appeared to recover synchronously and were then scored at designated time points. Post-dauer (PD) L4 worms were scored to determine whether P3.p had fused without dividing. To obtain *cwn-1(0); daf-7(ts)* PD L4 hermaphrodites, we performed SDS selection and plated dauers onto fresh OP50-seeded plates and allowed recovery to occur at 25°C. The SDS wash and fresh plating was sufficient to induce recovery, even at 25°C, although recovery was somewhat asynchronous. We picked PD L4 worms based on morphology and scored whether P3.p had fused without dividing.

To score LET-23::GFP in continuous and dauer life histories, we isolated eggs as described above and scored the population of larvae over time. In continuous development, L2-L3 molt worms were identified by picking non-pumping worms in lethargus. Constitutive 2-day dauers in this assay were not SDS-selected.

Imaging

Worms were immobilized in 10 mM levamisole on 3-4% agarose pads, unless otherwise noted. All fluorescence imaging was carried out using a Zeiss AxioObserver Z1 inverted spinning disk confocal microscope (Carl Zeiss) with a 63× oil objective.

ERK-nKTR was imaged using a dual camera setup such that red and green fluorescence were imaged simultaneously at the same exposure though a *z*-stack of 26 slices using 488 nm and 561 nm lasers. For comparison between stages, imaging parameters were modified between stages owing to differences in transgene brightness over time and data imaged at different parameters were normalized (see description of quantification below). For comparison at the same stage, imaging parameters were the same between control and experimental animals being imaged on the same day. For every ERK-nKTR experiment, we also captured ‘blank’ images for flat fielding using the same parameters. In general, dauer larvae were on their backs and ventral views were imaged.

Strains that did not contain ERK-nKTR were imaged using a single camera set up using either 488 nm or 561 nm lasers or both sequentially.

To image the Muv phenotype using differential interference contrast microscopy (Fig. 3D), we used a Zeiss Axio Imager Z1 microscope with a Hamamatsu Orca-ER camera and a 40× oil objective.

Development (2022) 149, dev201094. doi:10.1242/dev.201094

Quantification of ERK-nKTR (*arTi87* and *arTi85*)

Quantification of ERK-nKTR was carried out as described by de la Cova et al. (2017). However, we found that the baseline of the red/green ratio increases over time in dauer life history, and, as a consequence, the pixel by pixel red/green ratio calculated and scaled as described by de la Cova et al. (2017, 2020) did not give sufficient dynamic range. Therefore, we have instead reported upper quartile intensity (UQI) Nuclear Green/ UQI Nuclear Red, unscaled, which gives us greater dynamic range. Here, this is simply called 'red/green'.

To compare between developmental stages, the red/green value in P6.p was normalized to the red/green value for P4.p, a cell that does not normally have *mpk-1* activity, within each animal to look for differences in the pattern of ERK activity (de la Cova et al., 2017). Within the same stage, red/green values for a given VPC (P4.p or P6.p) were directly compared between mutants and controls. We excluded animals for which we were unable to use our pipeline to segment both P4.p or P6.p, for example because of worm movement.

Imaging and quantification of LET-23::GFP

To quantify LET-23::GFP protein localization, we adapted the method of Gauthier and Rocheleau (2021b). In order to compare basolateral and apical membranes, we only scored animals that were laying on their side (lateral view). To increase the number of dauers on their side, we decreased the concentration of agarose in the pad to 2% for that stage. We took 20 *z*-stack confocal images of P6.p in strains containing *zhIs035*. Using ImageJ, we created maximum intensity projections for each image, drew a thick line of a consistent width – about the size of the nucleus – through the center of the cell and collected the average GFP values across that line. This resulted in two peak values per cell, one at the apical and one at the basal membrane. These two peak fluorescence values were then used to determine the peak basal/apical fluorescence, giving one data point per animal. There were two settings used for experiments, one for imaging L2, L2/L3 molt and L3 and another for imaging L2d, the L2d-dauer molt and dauer, because we found that the apical expression in L3 gets so bright that we had to decrease laser power for continuous life history experiments.

Generation of *lin-3(ar656)* [LIN-3::SL2-nls::TdTomato::nls]

The endogenous LIN-3 transcriptional reporter was made using a self-excising drug selection cassette according to the protocol published by Dickinson et al. (2015) and using their published reagents. The 'sl2::nls::TdTomato::nls' insert was modeled after *lag-1*(*ar618*) (Luo et al., 2020). We used two previously unpublished plasmids, pKL142 and pKL143, made by Katherine Luo in our lab, that expressed the guide RNA and Cas9. The guide sequences were: GATCCCCGTCTCGAAGTTC and TCATTGGTTCACATGTTGC.

Generation of *arTi424* and *arTi425*, flexon-based reagents for expressing forms of LIN-3

In order to overexpress different forms of LIN-3 from the somatic gonad, we created miniMos single-copy insertion transgenes using the protocol described by Frøkjær-Jensen et al. (2014). Two plasmids were used to generate insertions. The first plasmid, pCO66, is designed to encode a synthetic signal sequence and the EGF domain as described by Katz et al. (1995). The second plasmid, pCO67, contains cDNA encoding the *lin-3* isoform 'S' as defined by Pu et al. (2017), and is based on the cDNA sequences from Van Buskirk and Sternberg (2007). Both plasmids contain the *rps-27* promoter, a form of LIN-3, and the *unc-54* 3′UTR cloned into the miniMos vector pCFJ1662, which also contains a hygromycin-resistance gene. Both pCO66 and pCO67 have the LIN-3 coding sequence interrupted by a *flexon* stop cassette as described by Shaffer and Greenwald (2022).

Two single-copy miniMos transgenes, *arTi424* (from pCO66) and *arTi425* (from pCO67), were generated. The *flexon* prevents functional protein production in the absence of Cre recombinase. Each transgene was combined with *arTi237* (somatic gonad Cre), and, after excision of the artificial exon, strong expression of functional EGF or LIN-3(S) (via the *rps-27* promoter) results specifically in the somatic gonad and causes a Muv phenotype. We note that *arTi424* produces an incompletely penetrant phenotype in the absence of the Cre recombinase driver, and the phenotype is enhanced by the presence of Cre recombinase.

Quantification and statistical analysis

A summary of statistical tests and *P*-values can be found in Table S4. All plots and statistical analysis were performed in GraphPad Prism. Some of our data was not normally distributed so we performed non-parametric tests on all data. To compare normalized ERK activity across more than two stages or red/green values between more than two strains, we used a Kruskal–Wallis test with Dunn's multiple comparisons test. We also used this test to compare LET-23::GFP A/B ratio across more than two stages. To compare ERK activity (red/green) in P6.p (or P4.p) between two genotypes we used a Kolmogrov–Smirnov test. Data displayed on graph includes bars to show the median and interquartile range. Each point represents one animal. We used a Fisher's exact test to compare the P3.p fates in Fig. 6C. For experiments in which we did not normalize P6.p to P4.p, we only considered *P*-values <0.01 to be significant, although we noted in Table S4 all *P*-values <0.05 that were obtained. We chose this more stringent cutoff because there was some variability in the baseline values for each experiment when normalization was not able to be performed because the experimental conditions affecting intrinsic signaling would also affect P4.p.

Acknowledgements

We are indebted to Claire de la Cova for valuable advice on quantification of the ERK-nKTR and comments on this manuscript and to Xantha Karp for insightful discussions about dauer larvae. We also thank Barth Grant for helpful discussions about EGFR trafficking, Katherine Luo and Justin Shaffer for sharing strains and plasmids, and Alex Hajnal, Guangshuo Ou and Zhiwen Zhu for strains. Some strains were provided by the CGC, which is funded by NIH Office of Research Infrastructure Programs (P40 OD010440).

Competing interests

The authors declare no competing or financial interests.

Author contributions

Conceptualization: C.O., I.G.; Formal analysis: C.O.; Investigation: C.O.; Data curation: C.O.; Writing - original draft: C.O.; Writing - review & editing: C.O., I.G.; Visualization: C.O.; Supervision: I.G.; Project administration: I.G.; Funding acquisition: C.O., I.G.

Funding

This work was supported by the National Institute of General Medical Sciences (grants R35GM131746 to I.G. and F31GM126741 to C.O., and training grant T32GM008798 to C.O.). Deposited in PMC for release after 12 months.

References

Abdus-Saboor, I., Mancuso, V. P., Murray, J. I., Palozola, K., Norris, C., Hall, D. H., Howell, K., Huang, K. and Sundaram, M. V. (2011). Notch and Ras promote sequential steps of excretory tube development in C. elegans. *Development* **138**, 3545-3555. doi:10.1242/dev.068148

Attner, M. A., Keil, W., Benavidez, J. M. and Greenwald, I. (2019). HLH-2/E2A expression links stochastic and deterministic elements of a cell fate decision during C. elegans gonadogenesis. *Curr. Biol.* **29**, 3094-3100.e4. doi:10.1016/j.cub.2019.07.062

Baugh, L. R. and Hu, P. J. (2020). Starvation responses throughout the Caenorhabditis elegans life cycle. *Genetics* **216**, 837-878. doi:10.1534/genetics.120.303565

Beitel, G. J., Clark, S. G. and Horvitz, H. R. (1990). Caenorhabditis elegans ras gene let-60 acts as a switch in the pathway of vulval induction. *Nature* **348**, 503-509. doi:10.1038/348503a0

Berset, T. A., Hoier, E. F. and Hajnal, A. (2005). The C. elegans homolog of the mammalian tumor suppressor Dep-1/Scc1 inhibits EGFR signaling to regulate binary cell fate decisions. *Genes Dev.* **19**, 1328-1340. doi:10.1101/gad.333505

Braendle, C. and Félix, M.-A. (2008). Plasticity and errors of a robust developmental system in different environments. *Dev. Cell* **15**, 714-724. doi:10.1016/j.devcel.2008.09.011

C. elegans Deletion Mutant Consortium. (2012). large-scale screening for targeted knockouts in the Caenorhabditis elegans genome. *G3* **2**, 1415-1425. doi:10.1534/g3.112.003830

Cassada, R. C. and Russell, R. L. (1975). The dauerlarva, a post-embryonic developmental variant of the nematode Caenorhabditis elegans. *Dev. Biol.* **46**, 326-342. doi:10.1016/0012-1606(75)90109-8

Cui, M., Kim, E. B. and Han, M. (2006). Diverse chromatin remodeling genes antagonize the Rb-involved SynMuv pathways in C. elegans. *PLoS Genet.* **2**, e74. doi:10.1371/journal.pgen.0020074
Dalley, B. K. and Golomb, M. (1992). Gene expression in the Caenorhabditis elegans dauer larva: Developmental regulation of Hsp90 and other genes. *Dev. Biol.* **151**, 80-90. doi:10.1016/0012-1606(92)90215-3
Das, D., Seemann, J., Greenstein, D., Schedl, T. and Arur, S. (2022). Reevaluation of the role of LIP-1 as an ERK/MPK-1 dual specificity phosphatase in the C. elegans germline. *Proc. Natl. Acad. Sci. USA* **119**, e2113649119. doi:10.1073/pnas.2113649119
de la Cova, C., Townley, R., Regot, S. and Greenwald, I. (2017). A real-time biosensor for ERK activity reveals signaling dynamics during C. elegans cell fate specification. *Dev. Cell* **42**, 542-553.e4. doi:10.1016/j.devcel.2017.07.014
de la Cova, C. C., Townley, R. and Greenwald, I. (2020). Negative feedback by conserved kinases patterns the degradation of Caenorhabditis elegans Raf in vulval fate patterning. *Development* **147**, dev195941. doi:10.1242/dev.195941
Delattre, M. and Félix, M.-A. (2001). Polymorphism and evolution of vulval precursor cell lineages within two nematode genera, Caenorhabditis and Oscheius. *Curr. Biol.* **11**, 631-643. doi:10.1016/S0960-9822(01)00202-0
Dickinson, D. J., Pani, A. M., Heppert, J. K., Higgins, C. D. and Goldstein, B. (2015). Streamlined genome engineering with a self-excising drug selection cassette. *Genetics* **200**, 1035-1049. doi:10.1534/genetics.115.178335
Diogon, M., Wissler, F., Quintin, S., Nagamatsu, Y., Sookhareea, S., Landmann, F., Hutter, H., Vitale, N. and Labouesse, M. (2007). The RhoGAP RGA-2 and LET-502/ROCK achieve a balance of actomyosin-dependent forces in C. elegans epidermis to control morphogenesis. *Development* **134**, 2469-2479. doi:10.1242/dev.005074
Eisenmann, D. M., Maloof, J. N., Simske, J. S., Kenyon, C. and Kim, S. K. (1998). The beta-catenin homolog BAR-1 and LET-60 Ras coordinately regulate the Hox gene lin-39 during Caenorhabditis elegans vulval development. *Development* **125**, 3667-3680. doi:10.1242/dev.125.18.3667
Euling, S. and Ambros, V. (1996). Reversal of cell fate determination in Caenorhabditis elegans vulval development. *Development* **122**, 2507-2515. doi:10.1242/dev.122.8.2507
Fielenbach, N. and Antebi, A. (2008). C. elegans dauer formation and the molecular basis of plasticity. *Genes Dev.* **22**, 2149-2165. doi:10.1101/gad.1701508
Freed, D. M., Alvarado, D. and Lemmon, M. A. (2015). Ligand regulation of a constitutively dimeric EGF receptor. *Nat. Commun.* **6**, 7380. doi:10.1038/ncomms8380
Freed, D. M., Bessman, N. J., Kiyatkin, A., Salazar-Cavazos, E., Byrne, P. O., Moore, J. O., Valley, C. C., Ferguson, K. M., Leahy, D. J., Lidke, D. S. et al. (2017). EGFR ligands differentially stabilize receptor dimers to specify signaling kinetics. *Cell* **171**, 683-695.e18. doi:10.1016/j.cell.2017.09.017
Frøkjær-Jensen, C., Davis, M. W., Sarov, M., Taylor, J., Flibotte, S., LaBella, M., Pozniakovsky, A., Moerman, D. G. and Jorgensen, E. M. (2014). Random and targeted transgene insertion in Caenorhabditis elegans using a modified Mos1 transposon. *Nat. Methods* **11**, 529-534. doi:10.1038/nmeth.2889
Gauthier, K. and Rocheleau, C. E. (2017). C. elegans vulva induction: an in vivo model to study epidermal growth factor receptor signaling and trafficking. *Methods Mol. Biol.* **1652**, 43-61. doi:10.1007/978-1-4939-7219-7_3
Gauthier, K. D. and Rocheleau, C. E. (2021a). Golgi localization of the LIN-2/7/10 complex points to a role in basolateral secretion of LET-23 EGFR in the Caenorhabditis elegans vulval precursor cells. *Development* **148**, dev194167. doi:10.1242/dev.194167
Gauthier, K. D. and Rocheleau, C. E. (2021b). LIN-10 can promote LET-23 EGFR signaling and trafficking independently of LIN-2 and LIN-7. *Mol. Biol. Cell* **32**, 788-799. doi:10.1091/mbc.E20-07-0490
Gleason, J. E., Szyleyko, E. A. and Eisenmann, D. M. (2006). Multiple redundant Wnt signaling components function in two processes during C. elegans vulval development. *Dev. Biol.* **298**, 442-457. doi:10.1016/j.ydbio.2006.06.050
Golden, J. W. and Riddle, D. L. (1984). The Caenorhabditis elegans dauer larva: developmental effects of pheromone, food, and temperature. *Dev. Biol.* **102**, 368-378. doi:10.1016/0012-1606(84)90201-X
Haag, A., Gutierrez, P., Bühler, A., Walser, M., Yang, Q., Langouët, M., Kradolfer, D., Fröhli, E., Herrmann, C. J., Hajnal, A. et al. (2014). An in vivo EGF receptor localization screen in C. elegans Identifies the Ezrin homolog ERM-1 as a temporal regulator of signaling. *PLoS Genet.* **10**, e1004341. doi:10.1371/journal.pgen.1004341
Hajnal, A., Whitfield, C. W. and Kim, S. K. (1997). Inhibition of Caenorhabditis elegans vulval induction by gap-1 and by let-23 receptor tyrosine kinase. *Genes Dev.* **11**, 2715-2728. doi:10.1101/gad.11.20.2715
Hall, S. E., Beverly, M., Russ, C., Nusbaum, C. and Sengupta, P. (2010). A cellular memory of developmental history generates phenotypic diversity in C. elegans. *Curr. Biol.* **20**, 149-155. doi:10.1016/j.cub.2009.11.035
Hu, P. J. (2007). Dauer. *WormBook*. ed. The C. elegans Research Community, WormBook. doi/10.1895/wormbook.1.144.1, http://www.wormbook.org.
Hwang, B. J. and Sternberg, P. W. (2004). A cell-specific enhancer that specifies lin-3 expression in the C. elegans anchor cell for vulval development. *Development* **131**, 143-151. doi:10.1242/dev.00924
Jacobs, D., Beitel, G. J., Clark, S. G., Horvitz, H. R. and Kornfeld, K. (1998). Gain-of-function mutations in the Caenorhabditis elegans lin-1 ETS gene identify a C-terminal regulatory domain phosphorylated by ERK MAP kinase. *Genetics* **149**, 1809-1822. doi:10.1093/genetics/149.4.1809
Jacobs, D., Glossip, D., Xing, H., Muslin, A. J. and Kornfeld, K. (1999). Multiple docking sites on substrate proteins form a modular system that mediates recognition by ERK MAP kinase. *Genes Dev.* **13**, 163-175. doi:10.1101/gad.13.2.163
Jones, S. J. M., Riddle, D. L., Pouzyrev, A. T., Velculescu, V. E., Hillier, L. D., Eddy, S. R., Stricklin, S. L., Baillie, D. L., Waterston, R. and Marra, M. A. (2001). Changes in gene expression associated with developmental arrest and longevity in Caenorhabditis elegans. *Genome Res.* **11**, 1346-1352. doi:10.1101/gr.184401
Kaech, S. M., Whitfield, C. W. and Kim, S. K. (1998). The LIN-2/LIN-7/LIN-10 complex mediates basolateral membrane localization of the C. elegans EGF receptor LET-23 in vulval epithelial cells. *Cell* **94**, 761-771. doi:10.1016/S0092-8674(00)81735-3
Karp, X. (2018). Working with dauer larvae. *WormBook* ed. The C. elegans Research Community, WormBook. doi:10.1895/wormbook.1.180.1. http://www.wormbook.org.
Karp, X. and Ambros, V. (2012). Dauer larva quiescence alters the circuitry of microRNA pathways regulating cell fate progression in C. elegans. *Development* **139**, 2177-2186. doi:10.1242/dev.075986
Karp, X. and Greenwald, I. (2013). Control of cell-fate plasticity and maintenance of multipotency by DAF-16/FoxO in quiescent Caenorhabditis elegans. *Proc. Natl. Acad. Sci. USA* **110**, 2181-2186. doi:10.1073/pnas.1222377110
Katz, W. S., Hill, R. J., Clandinin, T. R. and Sternberg, P. W. (1995). Different levels of the C. elegans growth factor LIN-3 promote distinct vulval precursor fates. *Cell* **82**, 297-307. doi:10.1016/0092-8674(95)90317-8
Katz, W. S., Lesa, G. M., Yannoukakos, D., Clandinin, T. R., Schlessinger, J. and Sternberg, P. W. (1996). A point mutation in the extracellular domain activates LET-23, the Caenorhabditis elegans epidermal growth factor receptor homolog. *Mol. Cell. Biol.* **16**, 529-537. doi:10.1128/MCB.16.2.529
Klass, M. and Hirsh, D. (1976). Non-ageing developmental variant of Caenorhabditis elegans. *Nature* **260**, 523-525. doi:10.1038/260523a0
Larsen, P. L., Albert, P. S. and Riddle, D. L. (1995). Genes that regulate both development and longevity in Caenorhabditis elegans. *Genetics* **139**, 1567-1583. doi:10.1093/genetics/139.4.1567
Luo, K. L., Underwood, R. S. and Greenwald, I. (2020). Positive autoregulation of lag-1 in response to LIN-12 activation in cell fate decisions during C. elegans reproductive system development. *Development* **147**, dev193482. doi:10.1242/dev.193482
Maxeiner, S., Grolleman, J., Schmid, T., Kammenga, J. and Hajnal, A. (2019). The hypoxia-response pathway modulates RAS/MAPK-mediated cell fate decisions in Caenorhabditis elegans. *Life Sci. Alliance* **2**, e201800255. doi:10.26508/lsa.201800255
Mereu, L., Morf, M. K., Spiri, S., Gutierrez, P., Escobar-Restrepo, J. M., Daube, M., Walser, M. and Hajnal, A. (2020). Polarized epidermal growth factor secretion ensures robust vulval cell fate specification in Caenorhabditis elegans. *Development* **147**, dev175760. doi:10.1242/dev.175760
Miaczynska, M. (2013). Effects of membrane trafficking on signaling by receptor tyrosine kinases. *Cold Spring Harb. Perspect. Biol.* **5**, a009035. doi:10.1101/cshperspect.a009035
Miaczynska, M. and Bar-Sagi, D. (2010). Signaling endosomes: seeing is believing. *Curr. Opin. Cell Biol.* **22**, 535-540. doi:10.1016/j.ceb.2010.05.007
Miley, G. R., Fantz, D., Glossip, D., Lu, X., Saito, R. M., Palmer, R. E., Inoue, T., Van Den Heuvel, S., Sternberg, P. W. and Kornfeld, K. (2004). Identification of residues of the Caenorhabditis elegans LIN-1 ETS domain that are necessary for DNA binding and regulation of vulval cell fates. *Genetics* **167**, 1697-1709. doi:10.1534/genetics.104.029017
Myers, T. R. and Greenwald, I. (2007). Wnt signal from multiple tissues and lin-3/EGF signal from the gonad maintain vulval precursor cell competence in Caenorhabditis elegans. *Proc. Natl. Acad. Sci. USA* **104**, 20368-20373. doi:10.1073/pnas.0709989104
Nussinov, R., Tsai, C.-J. and Jang, H. (2021). Signaling in the crowded cell. *Curr. Opin. Struct. Biol.* **71**, 43-50. doi:10.1016/j.sbi.2021.05.009
Ogg, S., Paradis, S., Gottlieb, S., Patterson, G. I., Lee, L., Tissenbaum, H. A. and Ruvkun, G. (1997). The Fork head transcription factor DAF-16 transduces insulin-like metabolic and longevity signals in C. elegans. *Nature* **389**, 994–999. doi:10.1038/40194
Park, W.-Y., Park, J.-S., Cho, K.-A., Kim, D.-I., Ko, Y.-G., Seo, J.-S. and Park, S. C. (2000). Up-regulation of caveolin attenuates epidermal growth factor signaling in senescent cells. *J. Biol. Chem.* **275**, 20847-20852. doi:10.1074/jbc.M908162199
Parker, S., Walker, D. S., Ly, S. and Baylis, H. A. (2009). Caveolin-2 is required for apical lipid trafficking and suppresses basolateral recycling defects in the intestine of *Caenorhabditis elegans*. *Mol. Biol. Cell* **20**, 1763-1771. doi:10.1091/mbc.e08-08-0837
Platta, H. W. and Stenmark, H. (2011). Endocytosis and signaling. *Curr. Opin. Cell Biol.* **23**, 393-403. doi:10.1016/j.ceb.2011.03.008

Pu, P., Stone, C. E., Burdick, J. T., Murray, J. I. and Sundaram, M. V. (2017). The lipocalin LPR-1 cooperates with LIN-3/EGF signaling to maintain narrow tube integrity in Caenorhabditis elegans. *Genetics* **205**, 1247-1260. doi:10.1534/genetics.116.195156

Richardson, C. E., Yee, C. and Shen, K. (2019). A hormone receptor pathway cell-autonomously delays neuron morphological aging by suppressing endocytosis. *PLoS Biol.* **17**, e3000452. doi:10.1371/journal.pbio.3000452

Robinson-Thiewes, S., Dufour, B., Martel, P.-O., Lechasseur, X., Brou, A. A. D., Roy, V., Chen, Y., Kimble, J. and Narbonne, P. (2021). Non-autonomous regulation of germline stem cell proliferation by somatic MPK-1/MAPK activity in C. *elegans*. *Cell Rep.* **35**, 109162. doi:10.1016/j.celrep.2021.109162

Sato, K., Sato, M., Audhya, A., Oegema, K., Schweinsberg, P. and Grant, B. D. (2006). Dynamic regulation of Caveolin-1 trafficking in the germ line and embryo of *Caenorhabditis elegans*. *Mol. Biol. Cell* **17**, 3085-3094. doi:10.1091/mbc.e06-03-0211

Shaffer, J. M. and Greenwald, I. (2022). Floxed exon (Flexon): A flexibly positioned stop cassette for recombinase-mediated conditional gene expression. *Proc. Natl. Acad. Sci. USA* **119**, e2117451119. doi:10.1073/pnas.2117451119

Shin, H. and Reiner, D. J. (2018). The signaling network controlling C. elegans vulval cell fate patterning. *J. Dev. Biol.* **6**, E30. doi:10.3390/jdb6040030

Sigismund, S., Argenzio, E., Tosoni, D., Cavallaro, E., Polo, S. and Di Fiore, P. P. (2008). Clathrin-mediated internalization is essential for sustained EGFR signaling but dispensable for degradation. *Dev. Cell* **15**, 209-219. doi:10.1016/j.devcel.2008.06.012

Skorobogata, O., Escobar-Restrepo, J. M. and Rocheleau, C. E. (2014). An AGEF-1/Arf GTPase/AP-1 ensemble antagonizes LET-23 EGFR basolateral localization and signaling during C. elegans vulva induction. *PLoS Genet.* **10**, e1004728. doi:10.1371/journal.pgen.1004728

Sloan, D. E. and Bembenek, J. N. (2020). Endogenous expression and localization of CAV-1::GFP in C. elegans. *MicroPublication Biol.* **2020**, 10.17912/micropub.biology.000311. doi:10.17912/micropub.biology.000311

Snutch, T. P. and Baillie, D. L. (1983). Alterations in the pattern of gene expression following heat shock in the nematode *Caenorhabditis elegans*. *Can. J. Biochem. Cell Biol.* **61**, 480-487. doi:10.1139/o83-064

Sternberg, P. W. (2005). Vulval development. *WormBook*. ed. The *C. elegans* Research Community, WormBook, doi:10.1895/wormbook.1.6.1 http://www.wormbook.org.

Sundaram, M. V. (2004). Vulval development: the battle between Ras and Notch. *Curr. Biol.* **14**, R311-R313. doi:10.1016/j.cub.2004.03.052

Sundaram, M. (2006). RTK/Ras/MAPK signaling. *WormBook*.ed. The C. elegans Research Community, WormBook. doi:10.1895/wormbook.1.80.1 http://www.wormbook.org.

Sundaram, M. V. (2013). Canonical RTK-Ras-ERK signaling and related alternative pathways. *WormBook* ed. The C. elegans Research Community, WormBook. doi:10.1895/wormbook.1.80.2. http://www.wormbook.org.

Swanson, M. M. and Riddle, D. L. (1981). Critical periods in the development of the Caenorhabditis elegans dauer larva. *Dev. Biol.* 84, 27-40. doi:10.1016/0012-1606(81)90367-5

Underwood, R. S., Deng, Y. and Greenwald, I. (2017). Integration of EGFR and LIN-12/Notch signaling by LIN-1/Elk1, the Cdk8 kinase module, and SUR-2/Med23 in vulval precursor cell fate patterning in Caenorhabditis elegans. *Genetics* **207**, 1473-1488. doi:10.1534/genetics.117.300192

Van Buskirk, C. and Sternberg, P. W. (2007). Epidermal growth factor signaling induces behavioral quiescence in Caenorhabditis elegans. *Nat. Neurosci.* **10**, 1300-1307. doi:10.1038/nn1981

von Zastrow, M. and Sorkin, A. (2007). Signaling on the endocytic pathway. *Curr. Opin. Cell Biol.* **19**, 436-445. doi:10.1016/j.ceb.2007.04.021

Vowels, J. J. and Thomas, J. H. (1992). Genetic analysis of chemosensory control of dauer formation in Caenorhabditis elegans. *Genetics* **130**, 105-123. doi:10.1093/genetics/130.1.105

Yoon, C. H., Lee, J., Jongeward, G. D. and Sternberg, P. W. (1995). Similarity of sli-1, a regulator of vulval development in C. elegans, to the mammalian proto-oncogene c-cbl. *Science* **269**, 1102-1105. doi:10.1126/science.7652556

Zhang, X. and Greenwald, I. (2011). Spatial regulation of lag-2 transcription during vulval precursor cell fate patterning in Caenorhabditis elegans. *Genetics* **188**, 847-858. doi:10.1534/genetics.111.128389

Zhou, Y., Prakash, P., Gorfe, A. A. and Hancock, J. F. (2018). Ras and the plasma membrane: a complicated relationship. *Cold Spring Harb. Perspect. Med.* **8**, a031831. doi:10.1101/cshperspect.a031831

Zinovyeva, A. Y. and Forrester, W. C. (2005). The C. elegans Frizzled CFZ-2 is required for cell migration and interacts with multiple Wnt signaling pathways. *Dev. Biol.* **285**, 447-461. doi:10.1016/j.ydbio.2005.07.014

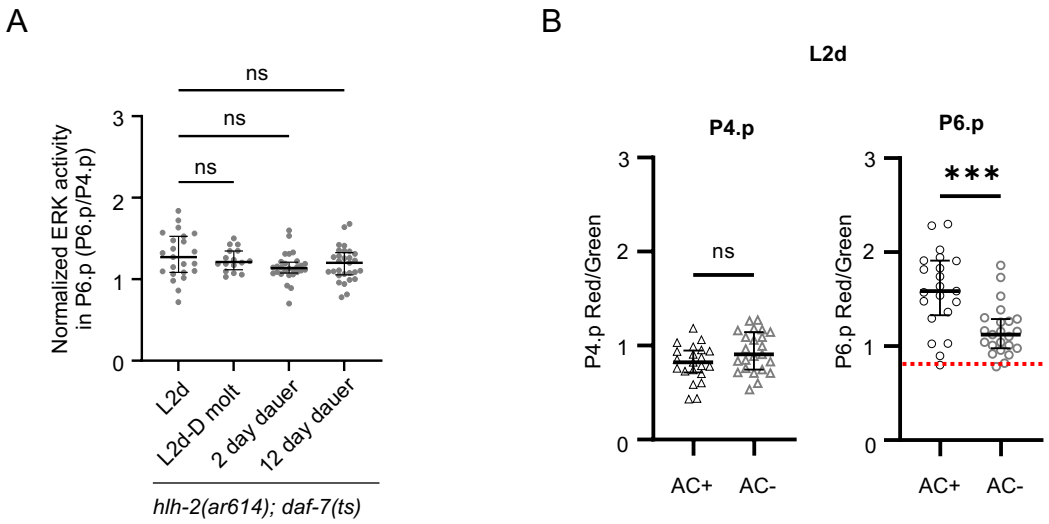

Fig. S1. Genetic ablation of the AC abrogates ERK activity in P6.p in L2d

These experiments show that normalized ERK activity in P6.p is indistinguishable at all stages in the absence of the AC (A) and that ERK activity in P6.p during L2d, like ERK activity in continuous development, depends on the inductive signal (B).

(A) Normalized ERK activity in P6.p at different stages in dauer life history when the AC is genetically ablated. *hlh-2(ar614)* mutants do not specify an AC and do not express the inductive signal (see Fig. S3C and Materials and Methods). ERK activity in P6.p was normalized to ERK activity in P4.p on a per-animal basis (P6.p/P4.p; grey solid circles) as the baseline increases over time (see Materials and Methods). L2d, n=23; L2-dauer molt, n=16; 2-day dauer, n=28; 12-day dauer, n=29. Genotype, *hlh-2(ar614)*; *daf-7(ts); ERK-nKTR.*

This strain was imaged in parallel with animals of genotype *hlh-2(+); daf-7(ts); ERK-nKTR* shown in Fig., 2B and at the same time points, and Red/Green values for P4.p and P6.p are directly compared in Fig. 2F and S1B using the same data.

(B) Comparison of ERK activity in P4.p (left, open triangles) and P6.p (open circles) in the presence or absence of the AC. The AC+ data are from the same L2d worms shown in Fig. 2B (n=31), and the AC- data are from the same L2d worms shown in S1A (n=28). The Red/Green ratio of each cell is not normalized to enable comparisons of the same cell at a given stage, as the baseline of expression of the ERK-nKTR is similar. The dashed red line represents the median Red/Green value in P4.p in AC+ animals during L2d to serve as a baseline reference.

Statistical Analysis: A: Kruskal-Wallis test with Dunn's multiple comparisons to compare L2d stages shown with a comparison line. B: Kolmogrov-Smirnov Test. P values: P<0.001 ***

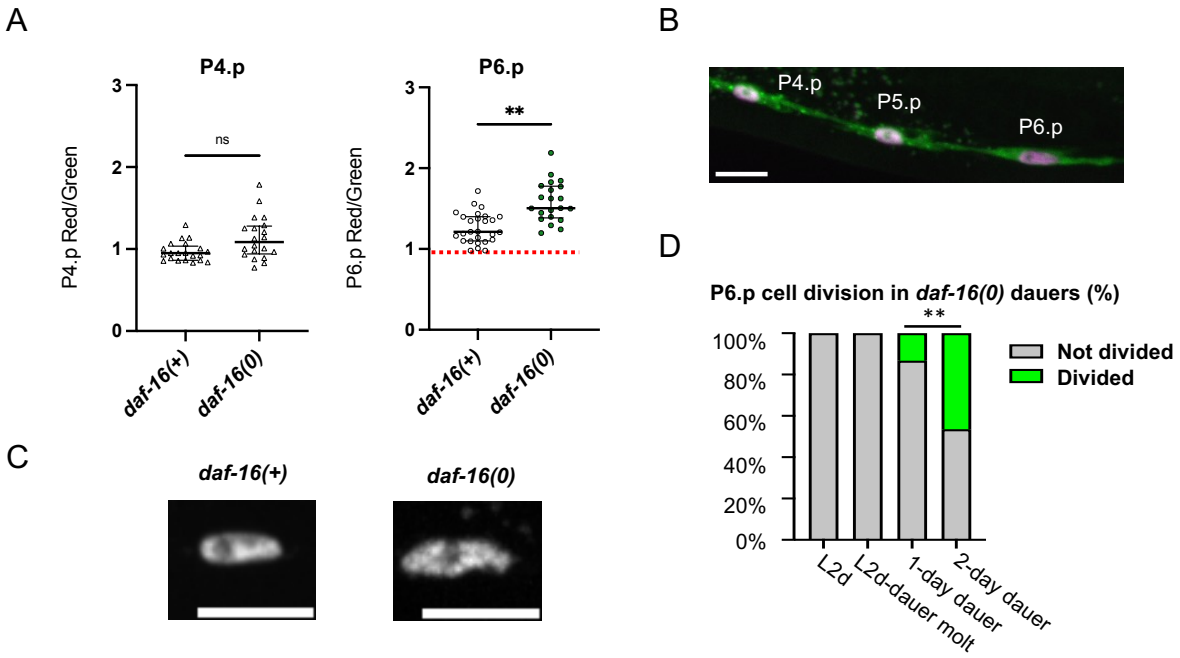

Fig. S2. Loss of *daf-16*/FOXO leads to increased ERK activity in P6.p in 1-day dauers

DAF-16/FOXO, the major downstream effector of the Insulin/Insulin-like signaling pathway, is required to maintain VPC multipotency and quiescence in dauer: in ~50% of *daf-16(0);daf-7* 2-day dauers, P6.p has divided and/or expressed the EGFR target gene *lag-2* (Karp and Greenwald, 2013). Here, we show that in *daf-16(0)* dauers, ERK activity is increased in P6.p in 1-day dauers, to capture VPCs before a substantial number had experienced changes to nuclear morphology that interfere with image quantification (see B) or had divided (see C).

(A) Comparison of ERK activity in P4.p (left, open triangles) and P6.p (right, open circles) in *daf-16(+)* vs *daf- 16(0)* dauers. The Red/Green ratio of each cell is not normalized to enable comparisons of the same cell at a given stage. The dashed red line represents the median Red/Green value in P4.p in *daf-16(+)* animals in 1-day dauers to serve as a baseline reference. We excluded 1-day *daf-16(0)* dauers in which nuclei have a "fragmented" appearance (see C). In some animals, P4.p had divided and the descendants have generally fused with hyp7, so neither P4.p nor its progeny was present for analysis (see D). Full genotypes: *daf-16(+); daf- 7(e1372ts); arTi87(ERK-nKTR)*, n=20 and *daf-16(mgDf50); daf-7(1372ts); arTi87(ERK-nKTR)*, n=17. *Statistical Analysis:* B: Kolmogrov-Smirnov Test. P values: P<0.01 ** P4.p p= 0.0293; P6.p p= 0.0015

(B) A 1-day SDS-selected dauer of genotype, *daf-16(mgDf50); daf-7(e1372ts); arTi87(ERK-nKTR)* shows visible reddening of the P6.p nucleus compared to P4.p and P5.p nuclei, indicative of a higher Red/Green ratio and ERK activity. Maximum intensity projection from confocal stack, images autoscaled in ImageJ (scale bar, 10 μm).

(C) In 2-day *daf-16(0)* dauers, mCherry::H2B often appears "fragmented" compared to the homogenous appearance in “wild-type” dauer nuclei, precluding the use of the Red value in a Red/Green ratio for these animals. Furthermore, expression from the *lin-31p* sequences decreases upon vulval induction (e.g. Shaffer and Greenwald, 2022), precluding a comparison of 1/Green values directly. In contrast, in 1-day dauers, mCherry::H2B appears largely homogeneous, allowing us to use a Red/Green ratio to obviate any concern about different levels of expression in different VPCs. The *daf-16(+)* image is representative of 2-day dauers and is from an experiment shown in Fig. 2B. Only the mCherry-H2B image is shown, maximum intensity projections of Z-stack images. Images autoscaled in ImageJ (scale bars, 10 μm).

(D) The proportion of *daf-16(0)* dauers in which P6.p has divided increases over time in dauer. For 1-day *daf- 16(0)* dauers, P6.p had divided in 23% of animals. In 2-day *daf-16(0)* dauers, the proportion increased to ~54%. L2d, n=17; the L2d-dauer molt, n=23; 1-day dauers, n=30; and 2-day dauers, n=28.

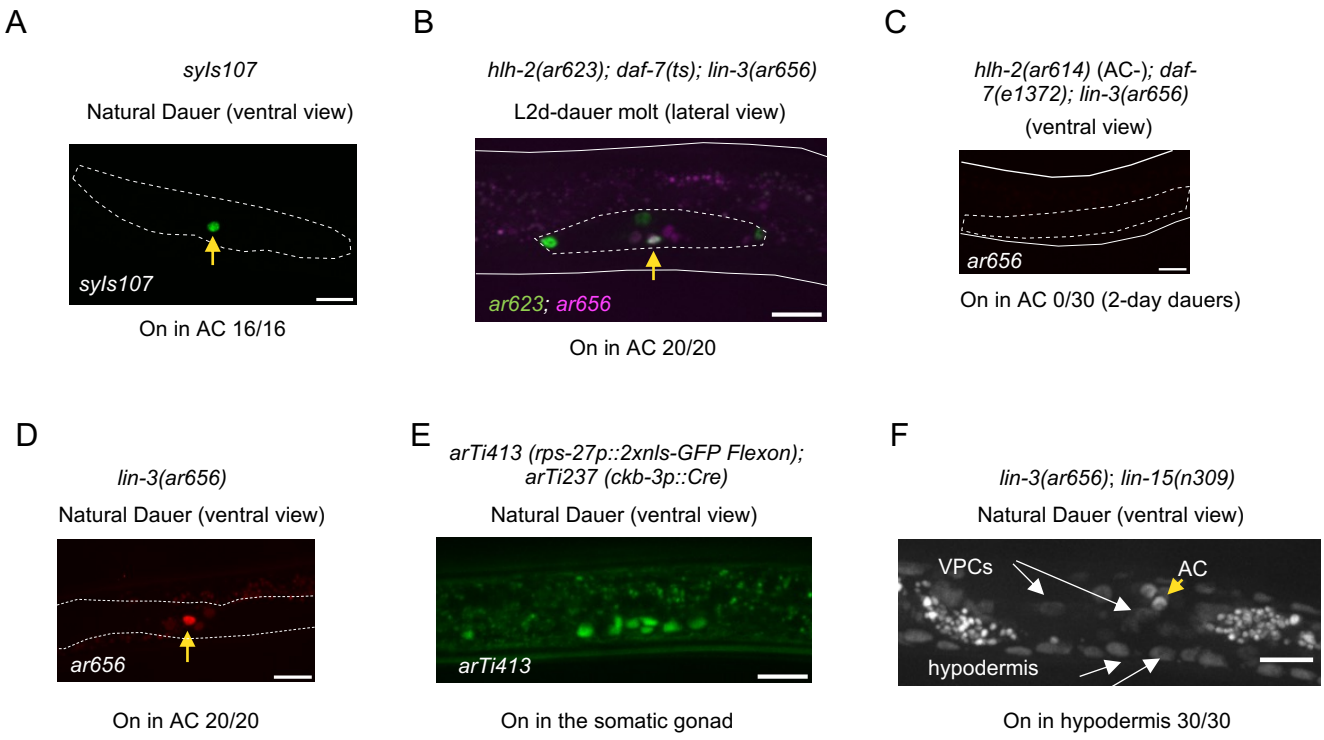

Fig. S3. Expression of the endogenous *lin-3*/EGF transcriptional reporter.

Dotted white lines outline the gonad, solid white lines outline the worm. Yellow arrows point to the Anchor Cell (AC). Images were autoscaled in ImageJ. All scale bars=10 μm.

(A) The *lin-3* transcriptional reporter *syIs107* [*lin-3(⊿pes-10)p::nls::GFP* + *unc-119(+)*] (Hwang and Sternberg, 2004) is expressed in the AC in SDS-selected natural dauers (n=16/16).

(B) *lin-3(ar656)* [*LIN-3::SL2::nls::TdTomato::nls*] is expressed in the AC during the L2d-dauer molt in *daf-7(ts)* worms (n=20/20). We note that at this stage, and in dauer larvae, there are some individuals in which expression of TdTomato in one VU is also bright, suggesting that the AC/VU decision may not have been fully resolved before dauer entry.

(C) *lin-3(ar656)* is not expressed in any proximal somatic gonadal cells in *hlh-2(ar614)* mutants (n=0/30), consistent with evidence that *lin-3* is a direct target of HLH-2/Daughterless in these cells (Hwang and Sternberg, 2004). SDS-selected 2-day dauers are shown. Expression of TdTomato is seen in other cells, as *hlh-2(ar614)* specifically abrogates HLH-2 expression in the proximal gonad (Attner et al., 2019).

(D) *lin-3(ar656)* is expressed in the AC in SDS-selected natural dauers (n= 20/20).

(E) Somatic gonad-specific expression of the *rps-27::gfp(flexon)* is observed in SDS-selected natural dauers upon excision of the *flexon* stop cassette when Cre is expressed in the somatic gonad precursors.

(F) In a *lin-15(n309)* background, *lin-3(ar656)* is expressed ectopically: TdTomato is readily visualized in the hyp7 hypodermal syncytium in SDS-selected dauers, which were made using the modified protocol for generating natural dauers (see Materials and Methods) (n=30/30).

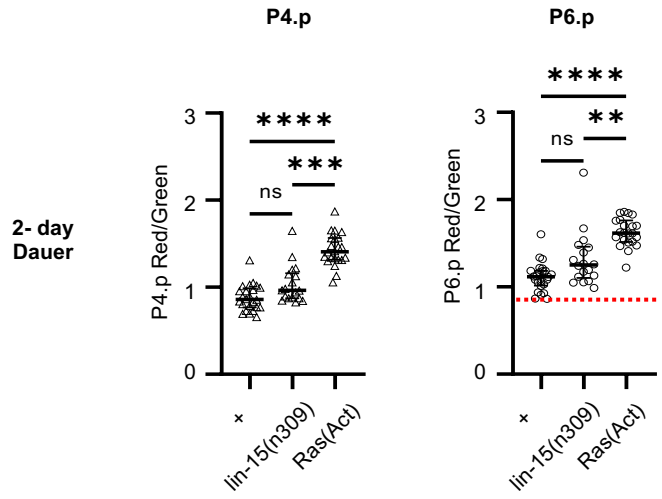

Fig. S4. ERK activity in Ras(Act) dauers is higher than in "wild-type" and *lin-15(n309)* 2-day dauers

ERK activity in P4.p (left) and P6.p (right) in *lin-15(n309)* and Ras(Act) mutants compared to wild-type [+, n=24; *lin-15(n309),* n=18; Ras(Act) n=22]. The dashed red line on the P6.p graph represents the median P4.p ERK activity value of the wild-type to serve as a baseline reference. The data for + and *lin-15(n309)* are also shown in Fig. 3F. Here we also show Ras(Act), which was scored in parallel, and compare all conditions as in Fig. 5D.

Statistical Analysis: Kruskal-Wallis test with Dunn's multiple comparisons to compare dauer genotypes shown with a comparison line. P values: P<0.01 **, P<0.001 ***, P<0.0001 ****

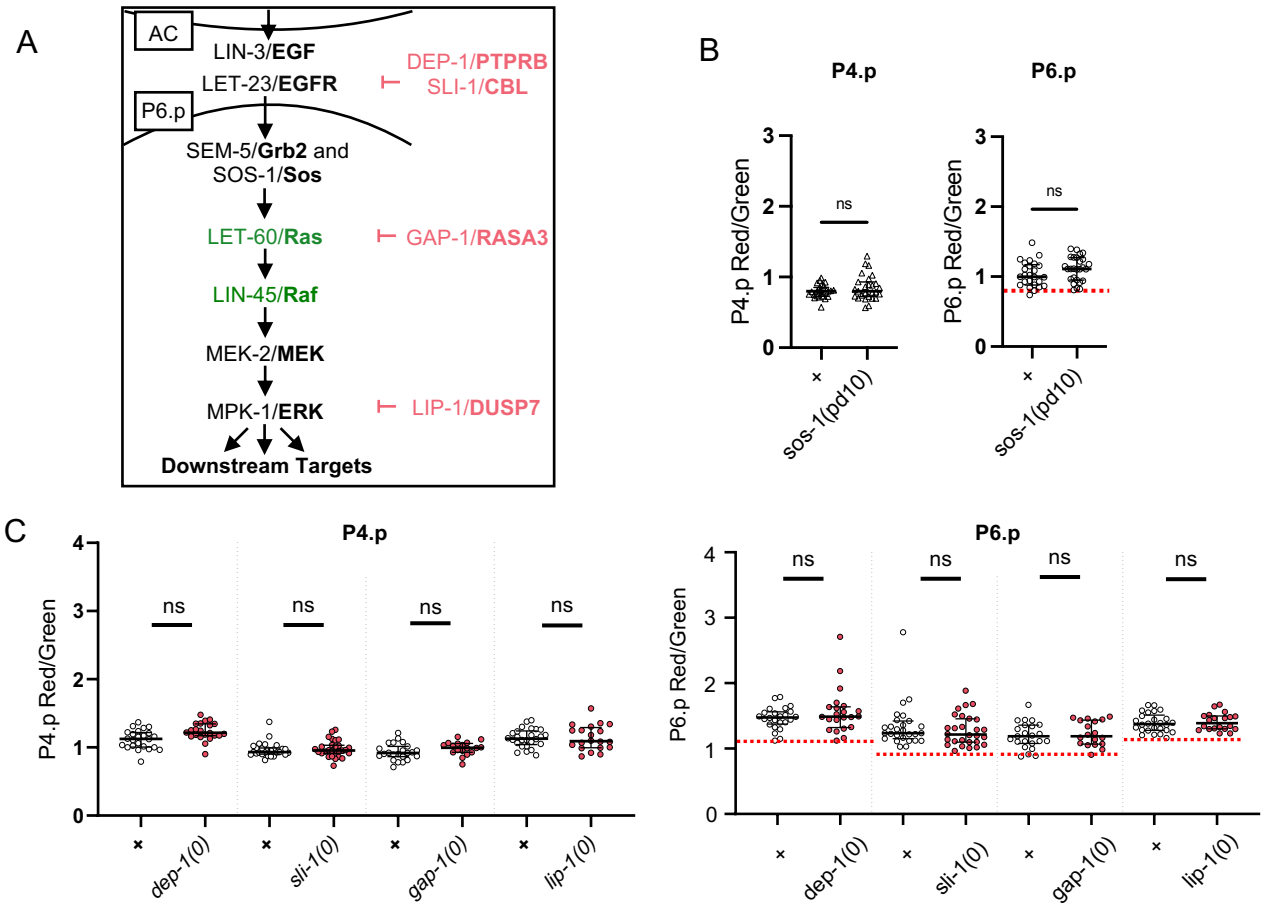

Fig. S5. Weakly activated SOS-1 and loss of known negative regulators of the EGFR pathway do not cause increased ERK activity in dauer VPCs

(A) Schematic of the EGFR signal transduction pathway and the steps at which select negative regulators act.

(B) Inconclusive results using the weakly hypermorphic allele *sos-1(pd10)*. As described in the main text, we contrasted the ability of a "strong" allele of *let-60* with the inability of a "strong" allele of *let-23* to activate ERK in P6.p to infer that ERK activity is opposed at or upstream of Ras activation. Importantly, these hypermorphic alleles all cause comparable, highly penetrant Multivulva (Muv) phenotypes in continuous development, so the difference in response in dauer is not simply attributable to the strength of the alleles.

SEM-5/Grb2 and SOS-1/Sos link the activation of LET-23/EGFR and LET-60/Ras in the VPCs. There are no alleles of *sem-5* that cause constitutive activity. The allele *sos-1(pd10)* was inferred to cause constitutive activity based on its ability to suppress a missense mutation in *sem-5*, although it was inferred to be only weakly active because it does not cause a Muv phenotype or a defect in another Ras-mediated cell fate decision in the excretory system (see Pu et al., 2017). This allele does not increase ERK activity in dauer larvae (B). Because the allele is weak, a negative result is not conclusive.

ERK activity in P4.p (left) and P6.p (right) between wild-type (n=25) and *sos-1(pd10)* (n=27) activating mutants. The dashed red line on the P6.p graph represents the median P4.p ERK activity value of the wild-type to serve as a baseline reference.

(C) Loss of individual negative regulators do not significantly increase ERK activity in dauer. Loss of individual negative regulators do not cause a Muv phenotype, but can suppress hypomorphic alleles of EGFR-Ras-ERK pathway components, in continuous development (reviewed in Sundaram, 2012).

ERK activity in P4.p (left) and P6.p (right) between wild-type and null alleles of negative regulators in dauer larvae, analyzed in parallel. + (n=24) vs *dep-1(zh34)* (n=22). + (n=27) vs *sli-1(sy143)* (n=28). + (n=23) vs *gap-1(ga133)* (n=18). + (n=26) vs *lip-1(ok154)* (n= 20).

Statistical Analysis: B and C: Kolmogrov-Smirnov Test to compare each mutant with ”wild-type” (+) from the same experiment. The P-value for + vs *dep-1(0)* in P4.p and + vs *gap-1(0)* in P4.p have P values <0.05, however, we only considered P-values <0.01 to be significant (see Materials and Methods).

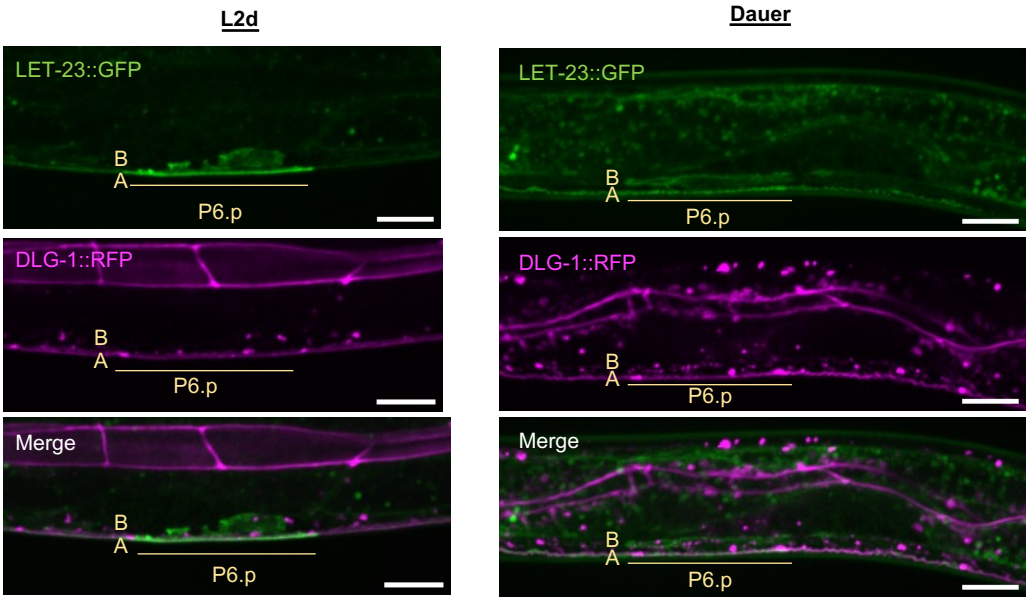

Fig. S6. Expression of LET-23::GFP and DLG-1::RFP in VPCs during L2d and in dauer

LET-23::GFP (*zhIs035*) is expressed on the basolateral ”B” and apical “A” membranes of P6.p in L2d and dauer larvae. DLG-1::RFP (*mcIs46*) localizes to *C. elegans* apical junctions (CeAJs) in epithelial cells and is present in both L2d and dauer larvae (Köppen et al., 2001; Labouesse, 2006; McMahon et al., 2001), indicating that VPCs maintain apical-basolateral polarity in dauer.

A

Genotype [all with *arTI87(ERK-nKTR)*]	**Dauer formation method**	**Time in dauer**	**# animals with P3.p fused/Total animals scored**	**Figure**
daf-7(ts)	*daf-7*	~2 days	0/30	2B
daf-7(ts)	*daf-7*	~12 days	0/33	2B
daf-2(ts)	*daf-2*	~2 days	0/30	2D
+	Starvation/Crowding ("Natural dauer")	Variable	1/25	6A
hlh-2(ar614); daf-7(ts)	*daf-7*	~2 days	0/32	2F
hlh-2(ar614); daf-7(ts)	*daf-7*	~12 days	0/34	S1A

B

EGF pathway mutant dauers [all with *daf-7(ts); arTi87(ERK-nKTR)*]	**# animals with P3.p fused/ Total animals scored**	**Figure**
LET-23(Act)	1/34	5A
LET-60(Act)	0/32	5A
LIN-45(Act)	0/31	5B
lin-15(n309)	0/30	3F
LIN-3(Flexon)	0/24	3E
EGF(Flexon)	1/33	3E

Fig. S7. Representative experiments showing that P3.p does not fuse with hyp7 in dauer larvae

In continuous development, P3.p fuses to hyp7 ~50% of the time in L2 without dividing. In contrast, P3.p almost never fuses in L2d prior to dauer entry or in dauer larvae. The ERK-nKTR was included in all backgrounds scored here to visualize if VPCs had fused or not (see Figure 6B). Data shown here comes from animals scored as part of experiments shown in the main text. See corresponding figures noted in the last column for each table.

(A) P3.p remained unfused to hyp7 throughout dauer in ~2-day dauers formed by *daf-7(ts)* or *daf-2(ts)* constitutive mutations, in older 12-day *daf-7(ts)* dauers, in "natural" dauers, and in animals lacking an AC (therefore also lacking EGF from the gonad).

(B) P3.p remained unfused to hyp7 in 2-day dauers in *let-60(n1046)* [Ras(Act)] or excess LIN-3/EGF activity [*lin-15(n309)*, LIN-3(Flexon), EGF(Flexon)]. Dauer formation was driven by *daf-7(ts)*.

Supplemental References:

Köppen, M., Simske, J. S., Sims, P. A., Firestein, B. L., Hall, D. H., Radice, A. D., Rongo, C. and Hardin, J. D. (2001). Cooperative regulation of AJM-1 controls junctional integrity in Caenorhabditis elegans epithelia. *Nat Cell Biol* **3**, 983–991.

Labouesse, M. (2006). Epithelial junctions and attachments. *WormBook* 1–21. The *C. elegans* Research Community, WormBook, doi/10.1895/wormbook.1.56.1, http://www.wormbook.org.

McMahon, L., Legouis, R., Vonesch, J. L. and Labouesse, M. (2001). Assembly of C. elegans apical junctions involves positioning and compaction by LET-413 and protein aggregation by the MAGUK protein DLG-1. *J Cell Sci* **114**, 2265–2277.

Table S1. *C. elegans* strains

Click here to download Table S1

Table S2. *C. elegans* transgenes

Allele	Description	Reference
arti87 X	*lin-31p::ERK-nKTR::unc-54 3'UTR* (Minimos)	de la Cova et al., 2020
arTi85 I	*lin-31p::ERK-nKTR::unc-54 3'UTR* (Minimos)	de la Cova et al., 2017
arti237 X	*ckb-3p::Cre-opti::tbb-2 3'UTR* (Minimos)	Shaffer and Greenwald, 2022
arTi424 IV	*rps-27p::LIN-3(EGF) Flexon::unc-54 3'UTR* (Minimos)	This work
arTi425 IV	*rps-27p:LIN-3(S) Flexon::unc-54 3-UTR* (Minimos)	This work
arTi31 IV	*lin-31p::lin-45(T432A,S436A,V627E)::unc-54 3'UTR* (Minimos)	de la Cova et al., 2017
zhIs035 I	*let-23::GFP + unc-119(+)*	Haag et al. 2014
mcIs46	*dlg-1::RFP + unc-119(+)*	Diogon et al., 2007 (CGC)
syIs107	*lin-3(delta pes-10)::GFP + unc-119(+)*	Hwang and Sternberg, 2004 (CGC)
arTi413 II	*rps-27p::2xnls-GFP Flexon::unc-54 3' UTR*	This work

Table S3. Plasmids

Allele	Description	Source	Additional Information	Generated
pCO66	*rps-27p::LIN-3(EGF) Flexon::unc-54 3'UTR* (Minimos)		MiniMos backbone pCFJ1662	*arTi424*
pCO67	*rps-27p:LIN-3(S) Flexon::unc-54 3-UTR* (Minimos)		MiniMos backbone pCFJ1662	*arTi425*
pCO68	Homology Repair Template C terminal: LIN-3::sl2::nls::TdTomato::nls with SEC cassette		with SEC cassette from (Dickinson et al. 2015)	*lin-3(ar656)*
pKL142	sgRNA *lin-3(ar656)* +Cas9	Katherine Luo		*lin-3(ar656)*
pKL143	sgRNA *lin-3(ar656)* +Cas9	Katherine Luo		*lin-3(ar656)*

Table S4. Statistics

Click here to download Table S4